



# Neutrophils Mediate Protection Against Colitis and Carcinogenesis by Controlling Bacterial Invasion and IL22 Production by $\gamma\delta$ T Cells

Silvia Carnevale<sup>1</sup>, Andrea Ponzetta<sup>1</sup>, Anna Rigatelli<sup>1</sup>, Roberta Carriero<sup>1</sup>, Simone Puccio<sup>1,2</sup>, Domenico Supino<sup>1</sup>, Giovanna Grieco<sup>1,3</sup>, Piera Molisso<sup>1,3</sup>, Irene Di Ceglie<sup>1</sup>, Francesco Scavello<sup>1</sup>, Chiara Perucchini<sup>1</sup>, Fabio Pasqualini<sup>1,3</sup>, Camilla Recordati<sup>4</sup>, Claudio Tripodo<sup>5</sup>, Beatrice Belmonte<sup>5</sup>, Andrea Mariancini<sup>1,3</sup>, Paolo Kunderfranco<sup>1</sup>, Giuseppe Sciumè<sup>6</sup>, Enrico Lugli<sup>1</sup>, Eduardo Bonavita<sup>1,3</sup>, Elena Magrini<sup>1</sup>, Cecilia Garlanda<sup>1,3</sup>, Alberto Mantovani<sup>1,3,7</sup>, and Sebastien Jaillon<sup>1,3</sup>

## ABSTRACT

Neutrophils are the most abundant leukocytes in human blood and play a primary role in resistance against invading microorganisms and in the acute inflammatory response. However, their role in colitis and colitis-associated colorectal cancer is still under debate. This study aims to dissect the role of neutrophils in these pathologic contexts by using a rigorous genetic approach. Neutrophil-deficient mice (*Csf3r*<sup>-/-</sup> mice) were used in classic models of colitis and colitis-associated colorectal cancer and the role of neutrophils was assessed by histologic, cellular, and molecular analyses coupled with adoptive cell transfer. We also performed correlative analyses using human datasets. *Csf3r*<sup>-/-</sup> mice showed increased susceptibility to colitis and colitis-associated colorectal cancer compared with control *Csf3r*<sup>+/+</sup> mice and adoptive transfer of neutrophils in *Csf3r*<sup>-/-</sup>

mice reverted the phenotype. In colitis, *Csf3r*<sup>-/-</sup> mice showed increased bacterial invasion and a reduced number of healing ulcers in the colon, indicating a compromised regenerative capacity of epithelial cells. Neutrophils were essential for  $\gamma\delta$  T-cell polarization and IL22 production. In patients with ulcerative colitis, expression of *CSF3R* was positively correlated with *IL22* and *IL23* expression. Moreover, gene signatures associated with epithelial-cell development, proliferation, and antimicrobial response were enriched in *CSF3R*<sup>high</sup> patients. Our data support a model where neutrophils mediate protection against intestinal inflammation and colitis-associated colorectal cancer by controlling the intestinal microbiota and driving the activation of an IL22-dependent tissue repair pathway.

## Introduction

Neutrophils are essential players in the innate immune response and represent the first line of defense against invading microorganisms (1). In addition to their antimicrobial effector functions, neutrophils have emerged as a crucial cell type in shaping immune and inflammatory responses in different pathologic conditions, including cancer (2, 3).

<sup>1</sup>IRCCS Humanitas Research Hospital, Rozzano, Milan, Italy. <sup>2</sup>Institute of Genetic and Biomedical Research, UoS Milan, National Research Council, Milan, Italy. <sup>3</sup>Department of Biomedical Science, Humanitas University, Pieve Emanuele, Milan, Italy. <sup>4</sup>Department of Veterinary Medicine and Animal Sciences, University of Milan, Mouse & Animal Pathology Laboratory (MAPLab), UniMi Foundation, Milan, Italy. <sup>5</sup>Tumor Immunology Unit, Department of Health Science, University of Palermo, School of Medicine, Palermo, Italy. <sup>6</sup>Department of Molecular Medicine, Sapienza University of Rome, Laboratory Affiliated to Istituto Pasteur Italia - Fondazione Cenci Bolognietti, Rome, Italy. <sup>7</sup>The William Harvey Research Institute, Queen Mary University of London, London, United Kingdom.

S. Carnevale and A. Ponzetta contributed equally to this article.

Current address for A. Ponzetta: Department of Medicine Huddinge, Center for Infectious Medicine, Karolinska Institutet, Stockholm, Sweden.

**Corresponding Author:** Sebastien Jaillon, Research Laboratory in Innate Immunity in Inflammation and Cancer, IRCCS Humanitas Research Hospital, Via Manzoni, 56, Rozzano, Milan 20089, Italy. E-mail: sebastien.jaillon@hunimed.eu

Cancer Immunol Res 2024;12:413–26

doi: 10.1158/2326-6066.CIR-23-0295

This open access article is distributed under the Creative Commons Attribution-NonCommercial-NoDerivatives 4.0 International (CC BY-NC-ND 4.0) license.

©2024 The Authors; Published by the American Association for Cancer Research

Colorectal cancer represents the third leading cause of cancer-related deaths worldwide (4). Patients with ulcerative colitis (UC) are at increased risk of developing colitis-associated colorectal cancer (CAC), which represents a cause of morbidity and death in these patients (5–8). The pathogenesis of CAC relies on different factors, including genetic alterations and environmental elements such as variations in the gut microbiota and mucosal healing (9–11).

Neutrophils have been proposed to affect the pathogenesis of inflammatory bowel disease (IBD)-associated colorectal cancer. However, both detrimental and beneficial effects of neutrophils have been reported and their overall role is still debated (12–21). For instance, neutrophils may be involved in limiting the presence of harmful microbiota (12, 14, 15) but, on the other hand, exacerbated neutrophilic inflammation has been reported to support IBD-associated colorectal cancer (17). These divergent results may reflect different methodologic approaches in studying the role of neutrophils [e.g., antibody-based depletion (13, 16, 17) versus genetically engineered mouse models impairing neutrophil survival or effector functions (12, 14, 15)]. Therefore, we decided to assess the role of neutrophils using a genetic model of neutrophil deficiency (*Csf3r*<sup>-/-</sup> mice, in which the production of neutrophils is dramatically reduced; ref. 22) complemented by adoptive cell transfer of neutrophils in classic models of dextran sodium sulfate (DSS)-induced colitis and azoxymethane (AOM)/DSS-induced CAC (23, 24).

Here, we report that neutrophil deficiency was associated with increased susceptibility to colitis and CAC. *Csf3r*<sup>-/-</sup> mice showed increased body weight loss, intestinal dysbiosis associated with increased bacterial invasion, and altered inflammatory responses. Histologic analysis revealed a reduced number of repairing ulcers in

*Csf3r*<sup>-/-</sup> mice, indicating that neutrophils sustained the regenerative capacity of colonic epithelial cells. In the intestine, the IL23/IL22 axis plays important roles in antimicrobial defense and mucosal healing (25–28). Consistent with these roles, we found that tissue levels of IL23 and IL22 were reduced in *Csf3r*<sup>-/-</sup> mice and adoptive cell transfer of neutrophils was sufficient to restore their expression. We found that neutrophil deficiency was associated with a selective impairment in the polarization and IL22 production of a subset of  $\gamma\delta$  T cells, both of which were restored by neutrophil adoptive transfer. Furthermore, we showed that neutrophils, through the control of intestinal microbiota, played a crucial role in the polarization of  $\gamma\delta$  T cells and protection against colitis.

In patients with UC, *CSF3R* expression was positively correlated with *IL22* and *IL23* expression. In addition, enrichment of epithelial repair and regeneration gene signatures were found in patients with higher *CSF3R* expression. Taken together, our data support a model where neutrophils control susceptibility to intestinal inflammation and CAC by shaping the intestinal microbiota composition and the activation of an IL22-dependent tissue repair pathway.

## Materials and Methods

### Animals

All mice used were on a C57BL/6J genetic background (RRID: IMSR\_JAX:000664). *Csf3r*-deficient (RRID:IMSR\_JAX:017838) and *Tcrd*<sup>-/-</sup> mice (RRID:IMSR\_JAX:002120) were purchased from The Jackson Laboratory. Colonies of wild-type mice (*Csf3r*<sup>+/+</sup>) and *Csf3r*<sup>-/-</sup> mice were generated from *Csf3r*<sup>+/+</sup> mice and were housed and bred in the SPF animal facility of Humanitas Clinical and Research Center in individually ventilated cages. Mice were randomized in experiments based on age and weight.

Procedures involving animals handling and care conformed to protocols approved by the Humanitas Clinical and Research Center in compliance with national (D.L. N.116, G.U., suppl. 40, 18–2-1992 and N.26, G.U. March 4, 2014) and international laws and policies (EEC Council Directive 2010/63/EU, OJ L 276/33, 22–09–2010; National Institutes of Health Guide for the Care and Use of Laboratory Animals, US National Research Council, 2011). The study was approved by the Italian Ministry of Health (approval n.261/2017-PR issued on 28/03/2017, no. 112/2019-PR issued on 12/02/2019 and approval no. 228/2023 issued on 17/03/2023). All efforts were made to minimize the number of animals used and their suffering. In most *in vivo* experiments, the investigators were unaware of the genotype of the experimental groups.

### Models of colitis and colitis-associated colorectal cancer

For the CAC model (AOM/DSS), 8-week-old female *Csf3r*<sup>+/+</sup> and *Csf3r*<sup>-/-</sup> mice were treated with AOM (Sigma-Aldrich, Catalog No. 25843–2; 10 mg/kg body weight) by intraperitoneal injection. After 7 days, mice received DSS (MP Biomedicals, Catalog No. 9011–18–1) 2.5% (w/v) in drinking water for 7 days. Then mice were allowed to recover for 14 days with normal drinking water. This schedule was repeated for four cycles. Body weight was monitored three times a week. For the acute colitis model, 8-week-old female *Csf3r*<sup>+/+</sup>, *Csf3r*<sup>-/-</sup>, and *Tcrd*<sup>-/-</sup> mice were treated with DSS 3% (w/v) in drinking water for 6 days. Mice were allowed to recover for 3 days with normal drinking water. Body weight was monitored daily. At the experimental endpoint, colon specimens were collected for histologic analysis, IHC, and cytokine measurements, or for flow cytometry analysis. In indicated colitis experiments, mice were intraperitoneally treated with 10  $\mu$ g/mouse of IL22 (BioLegend, Catalog No. 576208) or

with 50  $\mu$ g/mouse of specific mAb (Rat anti-IL22, Clone IL22JOP; Thermo Fisher Scientific; Rat Isotype Control, Clone eBR2a; Thermo Fisher Scientific) on days 2, 4, 6, and 8 after DSS administration.

### Neutrophil adoptive transfer

Neutrophils were isolated from the bone marrow of naïve *Csf3r*<sup>+/+</sup> mice and enriched using the Neutrophil Isolation Kit, mouse (Miltenyi Biotec).  $3 \times 10^6$  MACS-enriched bone marrow neutrophils (Purity  $\geq 97.5\%$ ) were injected intravenously in *Csf3r*<sup>-/-</sup> mice. On the basis of the calculated half-life of neutrophils in the intestine (29) and the period required for the normalization of the intestinal microbiota during cohousing (30), neutrophils were administered once a week for 30 days before the administration of DSS. Then, further neutrophil adoptive transfers were performed on days 0, 2, 6, and 8 with respect to DSS administration. To check for the presence of transferred neutrophils, we injected neutrophils in *Csf3r*<sup>-/-</sup> DSS-treated mice and collected blood and colon tissues 4 and 18 hours after neutrophil adoptive transfers. Tissues were processed and stained for flow cytometry analysis to assess for the presence of neutrophils.

### Histologic analysis and IHC

Colon specimens from DSS-treated *Csf3r*<sup>+/+</sup> and *Csf3r*<sup>-/-</sup> mice were collected. The surrounding fat tissue was removed, and the inner part of the colon washed extensively with PBS buffer to remove fecal material. Then, the tissues were placed in a histology cassette to form a Swiss roll and fixed with 4% formalin for 24 hours at room temperature. After dehydration with a series of ethanol solutions of increasing concentration, the Swiss rolls were paraffin embedded. FFPE Swiss rolls were analyzed for each condition. Tissue sections (4  $\mu$ m) were mounted on Super-frost slides, dewaxed in xylene, and rehydrated in ethanol, and then stained with hematoxylin (Histo-Line, Catalog No. 01HEMH1000) and eosin (H&E; Histo-Line, Catalog No. 01EOY101000) and evaluated by an expert veterinary pathologist to assess the colitis grade score according to the grading criteria in Supplementary Table S1. The presence of infiltrating bacteria (H&E staining), lymphoid structures (H&E staining), and follicular aggregates (*Mfge8*<sup>+</sup> RNAscope) was assessed by an expert pathologist. Mouse *Mfge8* transcript (Mm-Mfge8-C2; Cod. 408771-C2) was detected using RNAscope 2.5 HD Duplex Detection Reagents (Advanced Cell Diagnostic) in accordance with the manufacturer's instructions. Mm-Mfge8-C2 probe was diluted in RNAscope Probe Diluent (Cod.200041) and detected using AP Fast Red based reaction resulting in a red color. Slides were analyzed under a Zeiss AxioScope A1 and microphotographs were collected using a Zeiss Axiocam 503 Color with Zen 2.0 Software (Zeiss). For IHC, endogenous peroxidase was blocked for 20 minutes with 2% H<sub>2</sub>O<sub>2</sub> in PBS + 0.05% Tween 20. Antigen unmasking was performed in a decloaking chamber in EDTA pH 8.00 buffer (125°C for 3 minutes then 90°C for 5 minutes) for pSTAT3. Unspecific sites were blocked with Rodent Block M (Biocare Medical) for 30 minutes and tissues were incubated for 1 hours with monoclonal rabbit anti-pTyr 705 1:50 (clone D3A7, Cell Signaling Technology) in PBS+ 0.05% Tween 20. MACH1 Polymer Kit (Biocare Medical) was used as secondary antibody. 3,3'-Diaminobenzidine (DAB; Biocare Medical, Catalog No. DB801) was used as chromogen, then sections were counterstained with hematoxylin and mounted with Eukitt (Sigma-Aldrich, Catalog No. 25608–33–7) and analyzed with an Olympus BX51. The percentage of positive immunoreactive area for pSTAT3 was determined by Image ProAnalyzer software version 9.2 (Immagini&Computer). Ten fields were analyzed for each sample.

### Microflora depletion and cohousing

Eight-week-old mice were treated every day for 4 weeks by oral gavage with a cocktail of antibiotics: ampicillin (Pfizer) 10 mg/mL, vancomycin (PharmaTech Italia) 10 mg/mL, metronidazole (Società Prodotti Antibiotici) 5 mg/mL, and neomycin (Sigma-Aldrich) 10 mg/mL as described previously (31). Control mice were treated with drinking water. A gavage volume of 10 mL/kg (body weight) was delivered with a stainless-steel tube without prior sedation of mice. After 4 weeks of antibiotic treatment, mice started the AOM/DSS cycles or the DSS cycle, according to the procedures previously described (see Models of colitis and colitis-associated colorectal cancer). The antibiotic regimen was maintained until the experimental endpoint. DNA was isolated from bacterial fecal pellets, as described previously (31), collected before the antibiotic treatment and after the first cycle of DSS administration. PCR to detect the presence of 16S DNA was performed with 10 ng of DNA on two technical replicates using SybrGreen PCR Master Mix (Applied Biosystems) in a CFX96 Touch Real-Time PCR Detection System (Bio-Rad). The 16S primers were designed as described previously (31), and are listed in Supplementary Table S2. Data were analyzed with the  $2^{-(\Delta CT)}$  method, where the  $\Delta CT = (CT_{ABX} - CT_{NT})$ , and expressed as the percentage of the fold change (Applied Biosystems, Real-Time PCR Applications Guide). In cohousing experiments, pups from *Csf3r*<sup>+/+</sup> and *Csf3r*<sup>-/-</sup> mice were cohoused in the same cage (ratio 1:1) after weaning for 30 days before starting AOM/DSS or DSS treatments and were maintained in cohousing till the end of the experiment.

### Metagenomic analysis

DNA was isolated from bacterial fecal pellets with a PowerSoil DNA Isolation Kit (MO BIO Laboratories) and quantified by spectrophotometry at 260 nm. Next-generation sequencing (NGS) of 16S rRNA V3-V4 regions amplicons was carried out on a total of 15 samples. The samples were subjected to robotic PCR execution, library preparation and sequencing according to the Illumina 16S metagenomics standardized operational workflow (16S Metagenomic Sequencing Library Preparation, Part No. 15044223 Rev. B). Appropriate blanks (negative controls) and mock communities (positive control) were employed to assess bacterial contamination throughout the NGS workflow and sequencing error rate. Each 16S library was checked for size with an Agilent 2200 TapeStation (Agilent Technologies) and quantified with a Qubit 2.0 fluorometer using the Qubit dsDNA HS Assay Kit (Thermo Fisher Scientific, Catalog No. Q32851). Sequencing was performed at the Italian Institute of Technology (<https://www.iit.it/it/clns-sapienza>) with an Illumina MiSeq platform, Reagent Kit v3 (Catalog No. MS-102-3003, Illumina), 2 × 300 paired ends, and 600 cycles.

The 16S rRNA raw sequences were merged using Pandaseq and low-quality reads (i.e., showing stretches of bases with a quality score <20) were filtered out and discarded. Bioinformatic analyses were conducted using the QIIME2 software suite (release 2020.2), clustering filtered reads into operational taxonomic unit (OTU) at 97% identity level. Taxonomic assignment was performed via the RDP classifier against the SILVA database (32), with a 0.5 identity threshold. To compensate for different sequencing depths, all samples were rarefied to 1,000 reads. Bacterial biodiversity and distribution were characterized via  $\alpha$ - and  $\beta$ -diversity evaluations.  $\alpha$ -Diversity was measured through the QIIME pipeline using Shannon diversity metrics. Jaccard distance metrics were used to compare the microbial community structure in  $\beta$ -diversity analysis. Differential abundance (DA) analysis of microbiome data was identified with Analysis of Compositions of Microbiomes with Bias Correction (ANCOM) test 3.

### Cytokine measurement

Colon specimens of DSS-treated *Csf3r*<sup>+/+</sup> and *Csf3r*<sup>-/-</sup> mice were collected at day 9 (with respect to DSS administration) and were homogenized in 1 mL PBS containing protease inhibitors (Complete-EDTA-free; Roche) and PMSF (Sigma-Aldrich, Catalog No. 329-98-6; 1 mmol/L). Tissue homogenates were centrifuged at 14,000 rpm for 30 minutes at 4°C and supernatants were stored at -20°C for cytokine analysis. Murine IL22 (R&D DuoSet ELISA, Catalog No. DY582) and IL23 (R&D DuoSet, ELISA Catalogue No. DY1887) were measured in tissue homogenates by ELISA according to the manufacturer's instructions. Murine IL1 $\beta$ , IL4, IL5, IL6, IL10, IL17, IFN $\alpha$ , IFN $\beta$ , CXCL1, CXCL2, and CXCL10 were measured in tissue homogenates by ProcartaPlex assay custom panel (Thermo Fisher Scientific) according to the manufacturer's instructions.

### Coculture experiments

Bone marrow-derived macrophages (BMDM) were generated as described previously (22) and stimulated on day 7 with GM-CSF (50 ng/mL; Peprotech, Catalog No. 215-03), either alone or in combination with the TLR9 agonist CpG (250 nmol/L; Invivogen, Catalog No. tlr-1826) in RPMI1640 (Euroclone, Catalog No. ECB9006LX10) supplemented with 10% of FBS (Euroclone, Catalog No. ECS0186L), 1% of L-glutamine (BIO-CELL, Catalog No. ECS0186L), and 1% of penicillin/streptomycin (Euroclone, Catalog No. ECB3001D). In indicated conditions, BMDMs ( $1.5 \times 10^6$  cells) were cocultured with  $3 \times 10^5$  FACS-sorted neutrophils for 24 hours. Neutrophils were isolated from the bone marrow of naïve *Csf3r*<sup>+/+</sup> mice and enriched using the Neutrophil Isolation Kit, mouse (Miltenyi Biotec). MACS-enriched neutrophils were staining for FACS on a FACS-AriaIII (BD Biosciences) and sorted as CD45<sup>+</sup>CD11b<sup>+</sup>Ly6G<sup>+</sup> cells (purity >99.5%; anti-CD45 BV605, BD Biosciences, Catalog No. 563053; anti-CD11b APCCy7, BD Biosciences, Catalog No. 557657; anti-Ly6G PECF594, BD Biosciences, Catalog No. 562700). To block neutrophil production of ROS, neutrophils were pretreated with 10  $\mu$ mol/L of diphenyleneiodonium (DPI; Sigma-Aldrich, Catalog No. D2926) for 30 minutes at 37°C, then washed with RPMI1640 medium prior coculture. In transwell experiments, neutrophils were added into the upper compartment of a Transwell permeable support with 0.4  $\mu$ m pore (Corning). After coculture experiments, neutrophil viability was assessed with the Dead Cell Apoptosis Kits with Annexin V for Flow Cytometry (Thermo Fisher Scientific, Catalog No. V13242), according to the manufacturer's instructions. Cells were analyzed on a LSR Fortessa (BD Bioscience).

### Isolation of lamina propria cells and flow cytometry analysis

Colon specimens from DSS-treated *Csf3r*<sup>+/+</sup> and *Csf3r*<sup>-/-</sup> mice were manually disaggregated and then lamina propria cells (LPC) isolated using the Lamina Propria Cell Dissociation Kit (Miltenyi Biotec) and Gentle MACS Octo Dissociator (Miltenyi Biotec), according to the manufacturer's instructions. Flow cytometry procedures and instrument set up were carried out as described previously, with some modifications (33). Extracellular staining on LP single cell suspension or whole blood was performed using a PBS buffer containing 2% FBS, 2 mmol/L EDTA, and 0.05% NaN<sub>3</sub>. Prior to any surface staining, cells were incubated with Aqua LIVE/Dead-405 nm staining (Invitrogen) and negative cells were considered viable. Then Fc blocking reagent (Clone 24G2, eBioscience) was added to any cell suspension for 10 minutes at 4°C. Finally, an antibody mix was added to cell suspension for 20 minutes at 4°C and extracellular staining was performed. When needed, red blood cells lysis was performed with ACK lysis buffer (Euroclone) for 5 minutes at room temperature prior to fixation. All

murine antibodies used are listed in Supplementary Table S2. Foxp3/- Transcription Factor Staining Buffer Set (Thermo Fisher Scientific) was used for intracellular staining of transcription factors and cytokines. Cells were analyzed on a FACSymphony (BD Bioscience). Data were analyzed with FlowJo software version 10.8.2 (RRID: SCR\_008520; TreeStar).

### Ex vivo stimulation of LPCs

Cytokine stimulation experiments were performed on LPCs isolated from colon of DSS-treated *Csf3r*<sup>+/+</sup> and *Csf3r*<sup>-/-</sup> mice as described above [see Isolation of Lamina Propria Cells (LPC) and flow cytometry analysis]. LPCs were plated in 96-well plates at a density of  $1.5 \times 10^6$  cells/mL and cultured for 4 hours in RPMI1640 medium with 10% FBS, 1% L-glutamine, 1% Pen/Strep. The following cytokines were added in the indicated conditions: IL23 (100 ng/mL; Peprotech, Catalog No. 200-23) IL1 $\beta$  (50 ng/mL; Peprotech, Catalog No. 211-11B; ref. 16) or Cell Stimulation Cocktail 1 $\times$  (Thermo Fisher Scientific). BD Golgi-PlugTM (containing Brefeldin) was added 3 hours prior to intracellular staining.

### Analysis of public gene expression datasets

Gene expression datasets were retrieved from Gene Expression Omnibus (GEO, RRID:SCR\_005012) through their relative accession numbers. For the bulk RNA-sequencing dataset (GSE109142), we used TPM values from 206 patients. For the microarray gene set (GSE87473), gene expression profiles of 87 mucosal biopsies from adult patients with moderately to severely active UC were retrieved from GEO, in the form of RMA normalized intensity (log<sub>2</sub> transformation) normalized data. Data were imported in R (v3.1.1) and analyzed with R Bioconductor package *limma* (v3.50.1). “eBayes” *limma* function was applied to rank genes in order of evidence for differential expression, using an FDR  $\leq 0.05$ . Affymetrix Probe Set ID were annotated to mouse official gene symbols using the R Bioconductor package *pd.ht.hg.u133.plus.pm* (v3.12.0).

Gene correlation between *CSF3R* and expressed genes was performed using the *cor.test* function implemented in R (version 4.0.2) by the Spearman method. For both cohorts, *CSF3R* gene expression values were stratified by quartiles and patients belonging to the upper and lower quartiles were considered for differential expression analysis. Low and high *CSF3R* groups were used as input for differential expression test using the EdgeR package by the “glmQLFit” approach (version 3.30.3).

Gene set enrichment analysis (GSEA, version 3.0) was used to test for specific pathway enrichment in the high *CSF3R* group versus the low *CSF3R* group. The total gene lists were analyzed applying the “preranked” approach and the “classic” enrichment statistic method. Defined gene signatures were selected from MSigDB database choosing Reactome, Kegg and Gene Ontology as reference databases.

### Statistical analysis

Values were expressed as mean  $\pm$  SEM. Wilcoxon matched-pairs signed-rank test was used to compare the percentage of body weight loss between groups. Unpaired Student *t* test was used to compare groups with Gaussian distribution, two-tailed multiple Student *t* test was used to compare unmatched groups with Gaussian distribution. One-way ANOVA or Kruskal-Wallis test were used to compare multiple groups. Two-tailed Mann-Whitney *U* test was used to compare unmatched groups with non-Gaussian distribution. *P*  $\leq 0.05$  was considered significant. A ROUT test was applied to exclude outliers. Statistical analysis were calculated with GraphPad Prism version 9 (GraphPad Prism, RRID:SCR\_002798).

### Data availability

Data generated in this study are available in the manuscript and its supplementary files. All materials and any other data are available from the corresponding author upon reasonable request. Sequencing data generated in this study are available here (<https://zenodo.org/records/10047498> DOI: 10.5281/zenodo.10047498).

## Results

### Neutrophils mediate protection against CAC and colitis

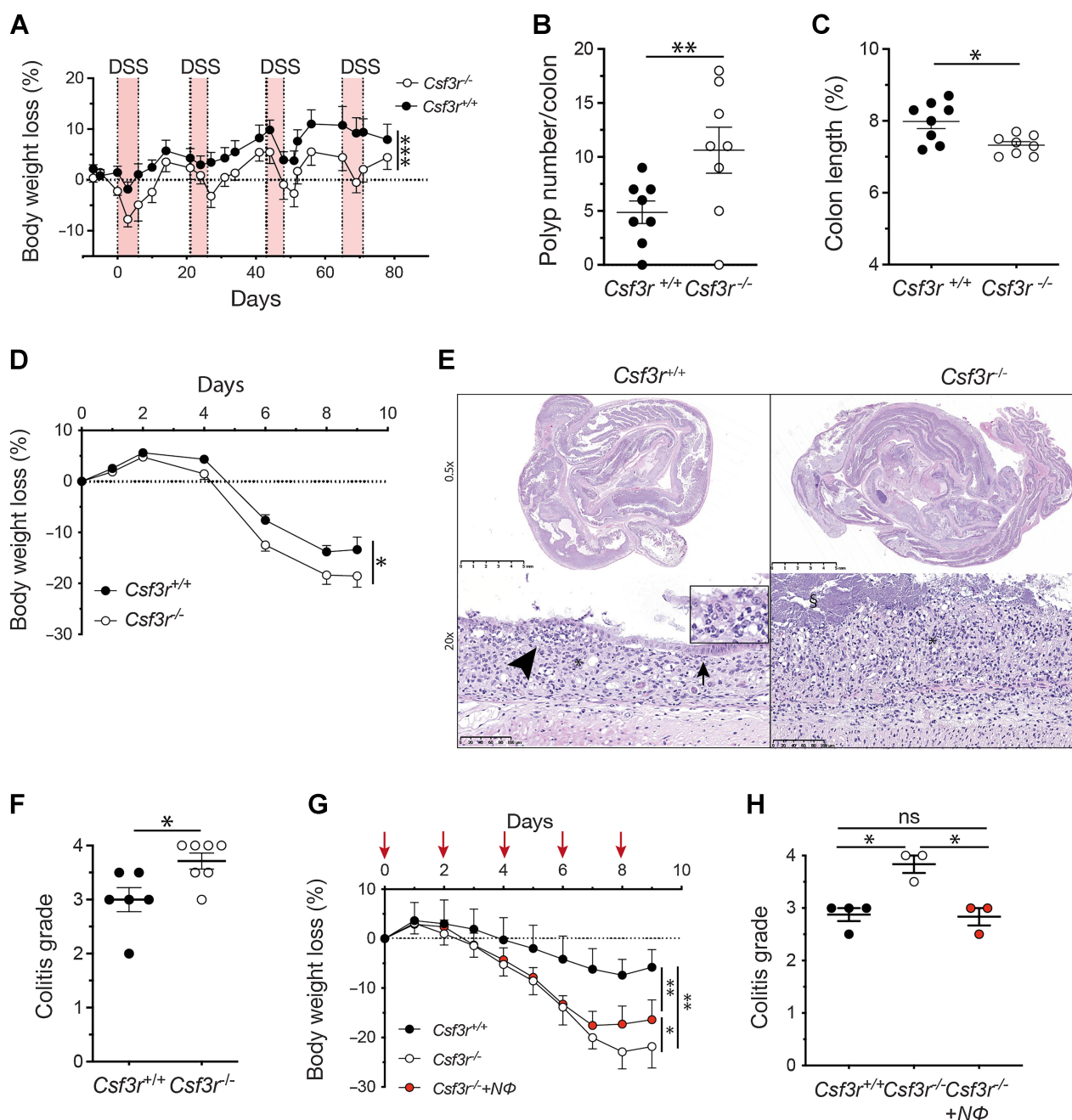
In the model of CAC (AOM/DSS), neutrophil deficient mice (*Csf3r*<sup>-/-</sup> mice) showed higher susceptibility to carcinogenesis, as indicated by increased body weight loss, higher polyp numbers, and shortened colon length compared with *Csf3r*<sup>+/+</sup> mice (Fig. 1A–C). Histologic analysis of colon tissue sections showed an increased number of total lymphoid structures and follicular aggregates (as indicated by the presence of Mfge8<sup>+</sup> dendritic cells; ref. 34) in *Csf3r*<sup>-/-</sup> colons, suggesting an altered inflammatory response in *Csf3r*<sup>-/-</sup> mice (Supplementary Figs. S1A–S1C).

Increased body weight loss was observed in *Csf3r*<sup>-/-</sup> mice as early as the first cycle of DSS administration (Fig. 1A), suggesting a protective role for neutrophils in colitis. Therefore, we assessed the impact of neutrophil deficiency in a widely used model of DSS-induced acute colitis [DSS 3% (w/v) in drinking water]. Higher body weight loss, and bacteria infiltration and colitis grade, both measured by histological analysis, indicated increased susceptibility to DSS-induced colitis in *Csf3r*<sup>-/-</sup> mice (Fig. 1D–F). Adoptive transfer of bone marrow-derived naïve neutrophils in *Csf3r*<sup>-/-</sup> mice prior to the administration of DSS was sufficient to reduce colitis severity (Fig. 1G and H). Of note, adoptively transferred neutrophils in *Csf3r*<sup>-/-</sup> mice were subsequently found in the bloodstream and reached the colon tissue (Supplementary Figs. S1D–S1F). Collectively, these data provide evidence that neutrophils mediate protection during CAC (Fig. 1A–C) and colitis (Fig. 1D–H).

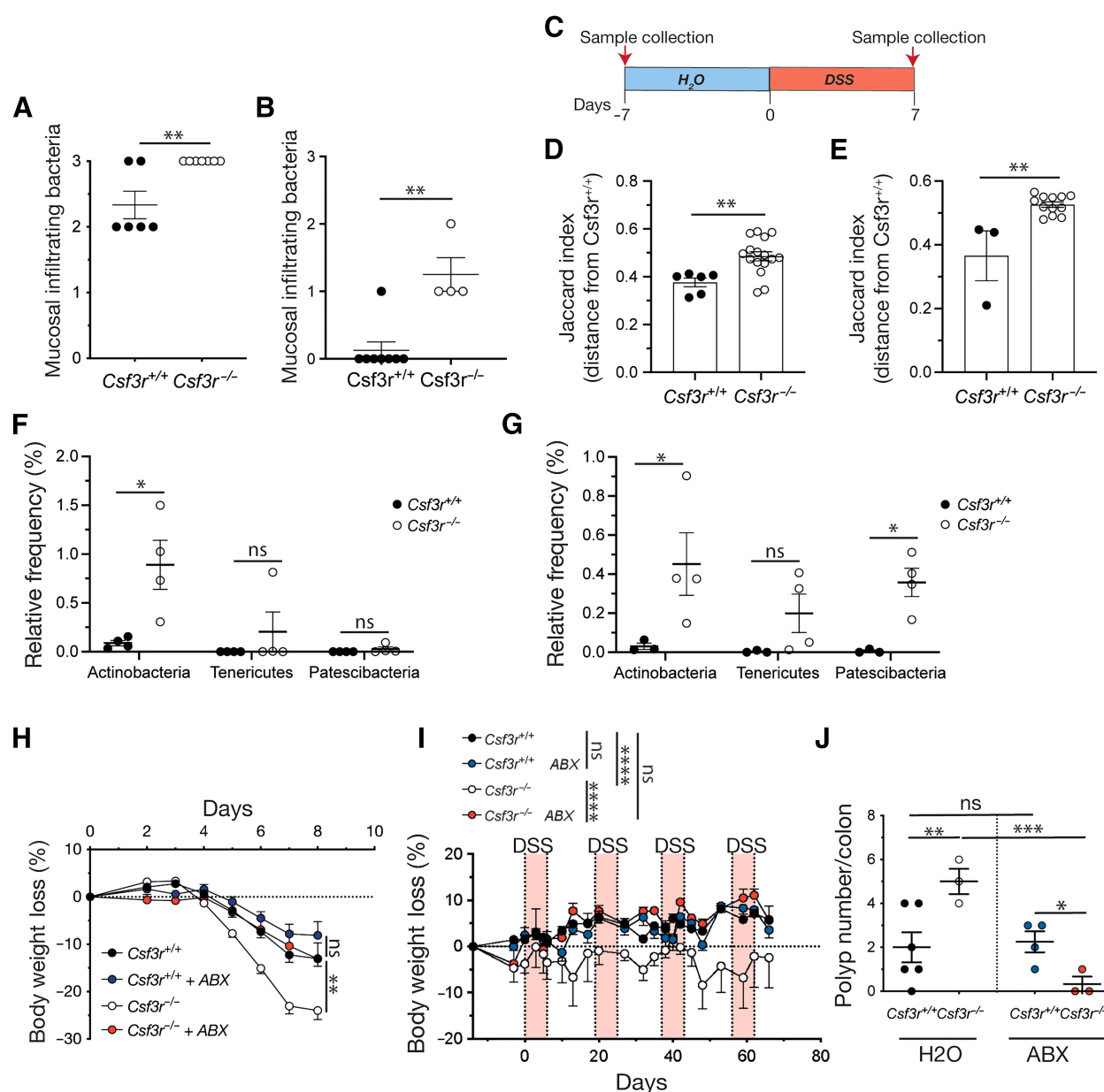
### Neutrophil deficiency is associated with intestinal dysbiosis and increased bacterial invasion

As observed in the model of DSS-induced acute colitis (Fig. 1E), histologic examination of colon tissue sections from mice treated with the AOM/DSS protocol showed increased bacterial invasion in the mucosa of *Csf3r*<sup>-/-</sup> mice, compared with *Csf3r*<sup>+/+</sup> mice (Fig. 2A and B; Supplementary Fig. S2A), indicating that neutrophils were involved in the control of the intestinal microbiota. Therefore, to assess whether neutrophil-mediated control occurred only upon inflammatory conditions or already at steady state, we characterized the microbiota composition of fecal samples collected from *Csf3r*<sup>-/-</sup> and *Csf3r*<sup>+/+</sup> mice before AOM/DSS administration (Day -7) and after the first cycle of DSS administration (Day 7; Fig. 2C).  $\alpha$  diversity analysis using Shannon index revealed no significant differences between *Csf3r*<sup>-/-</sup> and *Csf3r*<sup>+/+</sup> mice, indicating that the overall number of bacterial species was not affected by neutrophil deficiency (Supplementary Figs. S2B and S2C). In contrast,  $\beta$  diversity analysis using Jaccard index showed significant differences in the relative abundance of bacterial species at both day -7 and day 7 (Fig. 2D and E). Taxonomic analysis revealed a significantly increased frequency of *Actinobacteria* and *Patescibacteria*, along with a trend towards an increased frequency of *Tenericutes* in *Csf3r*<sup>-/-</sup> mice compared with *Csf3r*<sup>+/+</sup> mice (Fig. 2F and G; Supplementary Figs. S2D and S2E). Altogether, these findings showed that neutrophil deficiency resulted in an altered composition of the intestinal microbiota in both steady state and inflammatory conditions. Therefore, we examined the *in vivo*



**Figure 1.**

Neutrophil deficiency determines increased susceptibility to colitis-induced colorectal cancer and colitis. **A**, Percentage of body weight loss observed in *Csf3r*<sup>+/+</sup> ( $n = 8$ ) and *Csf3r*<sup>-/-</sup> ( $n = 8$ ) mice treated with AOM at day -7 and fed with DSS 2.5% as indicated by colored area. Polyp number observed macroscopically in the colon of *Csf3r*<sup>+/+</sup> ( $n = 8$ ) and *Csf3r*<sup>-/-</sup> ( $n = 8$ ) mice (B) and colon length at the experimental endpoint (C; day = 78). **D**, Percentage of body weight loss observed in *Csf3r*<sup>+/+</sup> ( $n = 11$ ) and *Csf3r*<sup>-/-</sup> ( $n = 10$ ) mice fed with DSS 3% from day 0 to day 6. **E**, Representative image from colon sections after DSS-induced colitis in *Csf3r*<sup>+/+</sup> and *Csf3r*<sup>-/-</sup> mice. \*, inflammation; §, bacteria; arrowhead, granulocytes (inset); arrow, re-epithelialization. **F**, Colitis grade in *Csf3r*<sup>+/+</sup> ( $n = 6$ ) and *Csf3r*<sup>-/-</sup> ( $n = 7$ ) mice fed with DSS 3% from day 0 to day 6. **G**, Percentage of body weight loss observed in *Csf3r*<sup>+/+</sup> ( $n = 10$ ), *Csf3r*<sup>-/-</sup> ( $n = 9$ ), and *Csf3r*<sup>-/-</sup> mice upon adoptive transfer of neutrophils (NΦ) received once a week for 4 weeks before the administration of DSS 3% and at day 0, 2, 6, and 8 after DSS administration ( $n = 8$ ). Days of treatment (2, 4, 6, 8) are indicated by red arrows. **H**, Colitis grade observed in *Csf3r*<sup>+/+</sup> ( $n = 4$ ), *Csf3r*<sup>-/-</sup> ( $n = 3$ ), and *Csf3r*<sup>-/-</sup> mice upon adoptive transfer of neutrophils (NΦ) received once a week for 4 weeks before the administration of DSS 3% and at day 0, 2, 6, and 8 after DSS administration ( $n = 3$ ). **A–C**, Representative data of three independent experiments; **D–F**, Representative data of five independent experiments; **G** and **H**, One experiment. **A, D, G**, Wilcoxon matched-pairs signed rank test. **B, C, F**, Unpaired Student *t* test. **K**, Kruskal–Wallis test. Data are mean ± SEM. \*,  $P < 0.05$ ; \*\*,  $P < 0.01$ ; \*\*\*,  $P < 0.001$ ; ns, not significant.

**Figure 2.**

Neutrophil deficiency is associated with altered intestinal microbiota composition. **A** and **B**, Quantification of infiltrating bacteria in colonic mucosa of *Csf3r<sup>+/+</sup>* and *Csf3r<sup>-/-</sup>* mice after one cycle of DSS administration (**A**; *Csf3r<sup>+/+</sup>* n = 6 and *Csf3r<sup>-/-</sup>* n = 7) or at the end of the AOM/DSS cycle (**B**; *Csf3r<sup>+/+</sup>* n = 8 and *Csf3r<sup>-/-</sup>* n = 4): absence = 0, focal = 1, multifocal = 2, disseminate = 3. **C**, Schematic representation of experimental setup for metagenomic analysis. **D** and **E**, Jaccard Distance showing the difference in the relative abundance of bacterial species in untreated (**D**) and DSS-treated (**E**) *Csf3r<sup>+/+</sup>* (untreated n = 4, DSS-treated n = 3) and *Csf3r<sup>-/-</sup>* (untreated n = 4, DSS-treated n = 4) mice. **F** and **G**, relative abundance of *Actinobacteria*, *Tenericutes* and *Patensibacteria* in *Csf3r<sup>+/+</sup>* and *Csf3r<sup>-/-</sup>* feces in untreated (**F**) and DSS-treated (**G**) mice. **H**, Body weight loss during DSS-induced acute colitis in *Csf3r<sup>+/+</sup>* (n = 7) and *Csf3r<sup>-/-</sup>* (n = 7) mice with and without antibiotic (ABX) oral treatment (*Csf3r<sup>+/+</sup>* + ABX n = 7 and *Csf3r<sup>-/-</sup>* + ABX n = 6). **I**, Body weight loss of AOM/DSS treated *Csf3r<sup>+/+</sup>* (n = 6) and *Csf3r<sup>-/-</sup>* (n = 3) mice with and without ABX oral treatment (*Csf3r<sup>+/+</sup>* + ABX n = 4 and *Csf3r<sup>-/-</sup>* + ABX n = 3). **J**, Macroscopic polyp count at the experimental endpoint (*Csf3r<sup>+/+</sup>* n = 6, *Csf3r<sup>+/+</sup>* + ABX n = 4, *Csf3r<sup>-/-</sup>* n = 3 and *Csf3r<sup>-/-</sup>* + ABX n = 3). **A–J**, One experiment. **A–E**, Unpaired Student *t* test. **F, G, J**, Multiple Student *t* test. **H** and **I**, Wilcoxon matched-pairs signed rank test. Data are mean ± SEM. \*, *P* < 0.05; \*\*, *P* < 0.01; \*\*\*, *P* < 0.001; ns, not significant.

relevance of the altered intestinal microbiota composition observed in *Csf3r<sup>-/-</sup>* mice in relation to their increased susceptibility to colitis and CAC. Both the administration of broad-spectrum antibiotics (Supplementary Fig. S2F) and the cohousing of *Csf3r<sup>+/+</sup>* and *Csf3r<sup>-/-</sup>* mice, which represents a widely accepted method for normalizing the

intestinal microbiota (30, 35), were sufficient to significantly reduce the pathological signs of both DSS-induced colitis (Fig. 2H; Supplementary Fig. S2G) and AOM/DSS-induced CAC in *Csf3r<sup>-/-</sup>* mice (Fig. 2I and J; Supplementary Figs. S2H and S2I). Conversely, we did not observe any effect of these treatments in *Csf3r<sup>+/+</sup>* mice, which have

neutrophils and are fully immunocompetent, as reported previously (14). Altogether, these results indicate that the intestinal dysbiosis we observed in *Csf3r*<sup>-/-</sup> mice was associated with increased susceptibility to colitis and CAC.

### IL22-dependent tissue repair response is impaired in *Csf3r*<sup>-/-</sup> mice during colitis

As mentioned above, we hypothesized that the increased susceptibility to colitis observed in *Csf3r*<sup>-/-</sup> mice was associated with an

altered inflammatory response. Histologic examination of colon tissue sections revealed a reduction in the number of healing ulcers in *Csf3r*<sup>-/-</sup> mice compared with *Csf3r*<sup>+/+</sup> mice (2/7 and 6/6, respectively), whereas the number of total ulcers was not affected by neutrophil deficiency (Fig. 3A; Supplementary Fig. S3A). The lower number of healing ulcers in *Csf3r*<sup>-/-</sup> mice indicated a defect in intestinal tissue repair. As the balance between inflammation and tissue repair is essential for the protection against colitis (36), we examined the levels of inflammatory cytokines in colon tissues of DSS-treated *Csf3r*<sup>-/-</sup> and

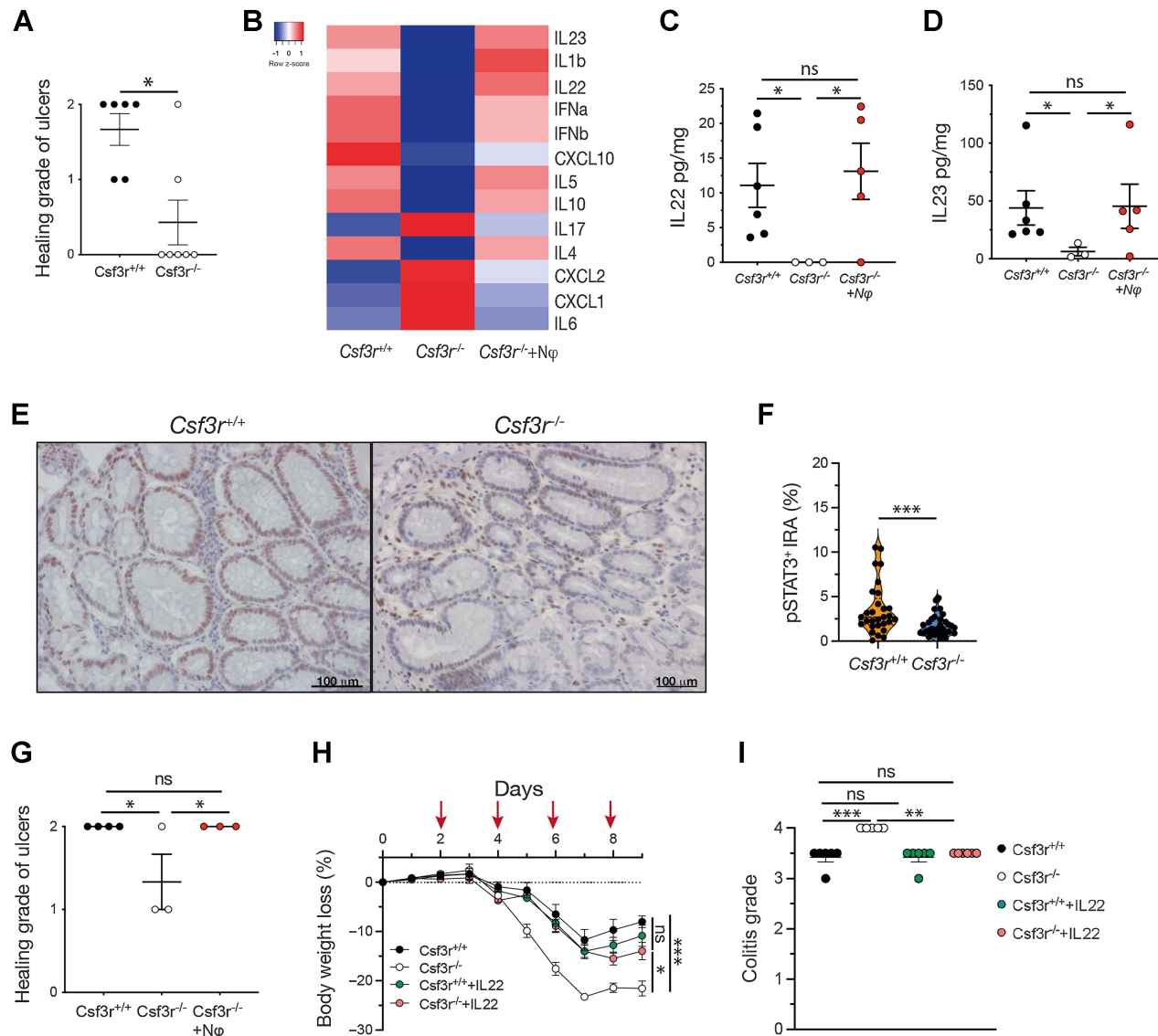


**Figure 3.**

Neutrophils mediate tissue repair and expression of IL23 and IL22 following colitis. **A**, Grade of healing of ulcers in colon tissues of DSS-treated mice assessed by an expert pathologist. *Csf3r*<sup>+/+</sup> (*n* = 6) and *Csf3r*<sup>-/-</sup> mice (*n* = 7) were treated with DSS in drinking water for 6 days and allowed to recover for 3 days with normal drinking water. Absent = 0, early re-epithelialization = 1, complete re-epithelialization = 2. **B**, Heatmap representing cytokine levels in colon tissues of DSS-treated *Csf3r*<sup>+/+</sup> (*n* = 6) and *Csf3r*<sup>-/-</sup> mice (*n* = 3) and *Csf3r*<sup>-/-</sup> mice upon adoptive transfer of neutrophils (Np; *n* = 5). **C** and **D**, IL22 (**C**) and IL23 (**D**) tissue levels in colon homogenates of DSS-treated *Csf3r*<sup>+/+</sup> (*n* = 6) and *Csf3r*<sup>-/-</sup> mice and *Csf3r*<sup>-/-</sup> mice (*n* = 3) upon adoptive transfer of neutrophils (Np; *n* = 5). **E**, Immunostaining analysis for pSTAT3 in colon tissues of DSS-treated mice (*Csf3r*<sup>+/+</sup>, *Csf3r*<sup>-/-</sup>, and *Csf3r*<sup>-/-</sup> + Np). **F**, pSTAT3 immunoreactive area (IRA) determined with a computer-assisted image analysis system. **G**, Grade of healing of ulcers in colon tissues of DSS-treated mice (*Csf3r*<sup>+/+</sup>, *Csf3r*<sup>-/-</sup>, and *Csf3r*<sup>-/-</sup> + Np). **H**, Percentage of body weight loss during DSS-induced acute colitis in *Csf3r*<sup>+/+</sup> (*n* = 6) and *Csf3r*<sup>-/-</sup> (*n* = 5) mice treated or not with IL22 (10 µg/mouse) via intraperitoneal injection [*Csf3r*<sup>+/+</sup> + IL22 (*n* = 6) and *Csf3r*<sup>-/-</sup> + IL22 (*n* = 6)]. Days of treatment (2, 4, 6, 8) are indicated by red arrows. **I**, Colitis grade observed in *Csf3r*<sup>+/+</sup> (*n* = 6) and *Csf3r*<sup>-/-</sup> (*n* = 5) mice treated or not with IL22 (10 µg/mouse) via intraperitoneal injection as indicated in **H** [*Csf3r*<sup>+/+</sup> + IL22 (*n* = 6) and *Csf3r*<sup>-/-</sup> + IL22 (*n* = 6)]. **A**, **F**, Unpaired Student *t* test. **H**, Wilcoxon matched-pairs signed rank test. **B**–**D**, **G**–**I**, Kruskal–Wallis test. Data are mean ± SEM. \*, *P* < 0.05; \*\*, *P* < 0.01; \*\*\*, *P* < 0.001; ns, not significant.

**Table 1.** Tissue levels of cytokines in colon homogenates from DSS-treated *Csf3r*<sup>+/+</sup> and *Csf3r*<sup>-/-</sup> mice.

	Colon homogenates (pg/ $\mu$ g tissue $\pm$ SEM)			Colon homogenates (pg/ $\mu$ g tissue $\pm$ SEM)		
	<i>Csf3r</i> <sup>+/+</sup> (n = 6)	<i>Csf3r</i> <sup>-/-</sup> (n = 3)	P value	<i>Csf3r</i> <sup>-/-</sup> (n = 3)	<i>Csf3r</i> <sup>-/-</sup> +N $\Phi$ (n = 5)	P value
IL10	0.7841 $\pm$ 0.2024	0.2599 $\pm$ 0.0877	0.0312 <sup>a</sup>	0.2599 $\pm$ 0.0877	0.7156 $\pm$ 0.2149	0.0510
IL4	0.1319 $\pm$ 0.0250	0.0528 $\pm$ 0.0106	0.0194 <sup>a</sup>	0.0528 $\pm$ 0.0106	0.1257 $\pm$ 0.0341	0.0533
IL5	0.4517 $\pm$ 0.0872	0.1978 $\pm$ 0.0388	0.0343 <sup>a</sup>	0.1978 $\pm$ 0.0388	0.4534 $\pm$ 0.1046	0.0204 <sup>a</sup>
IL6	9.807 $\pm$ 3.048	414.4 $\pm$ 154.6	0.0028 <sup>a</sup>	414.4 $\pm$ 154.6	37.18 $\pm$ 13.54	0.1345
CXCL10	4.05 $\pm$ 0.9019	1.726 $\pm$ 0.1962	0.0636	1.726 $\pm$ 0.1962	2.609 $\pm$ 0.5774	0.4325
CXCL-2	16.82 $\pm$ 6.218	91.21 $\pm$ 44.82	0.2234	91.21 $\pm$ 44.82	44.66 $\pm$ 16.71	0.9461
CXCL-1	2.571 $\pm$ 0.4314	196.4 $\pm$ 93.04	0.0014 <sup>a</sup>	196.4 $\pm$ 93.04	29.8 $\pm$ 9.612	0.4510
IFN $\alpha$	9.509 $\pm$ 1.477	3.717 $\pm$ 0.7656	0.0102 <sup>a</sup>	3.717 $\pm$ 0.7656	8.182 $\pm$ 2.062	0.0424 <sup>a</sup>
IFN $\beta$	4.253 $\pm$ 0.8373	2.189 $\pm$ 0.6985	0.0335 <sup>a</sup>	2.189 $\pm$ 0.6985	3.779 $\pm$ 1.037	0.0985
IL23	43.97 $\pm$ 14.91	6.242 $\pm$ 3.71	0.0425 <sup>a</sup>	6.242 $\pm$ 3.71	45.38 $\pm$ 19.09	0.0382 <sup>a</sup>
IL22	11.09 $\pm$ 3.165	n.d.	0.0403 <sup>a</sup>	n.d.	13.12 $\pm$ 4.043	0.0244 <sup>a</sup>
IL1 $\beta$	23.94 $\pm$ 2.245	6.674 $\pm$ 2.189	0.0208 <sup>a</sup>	6.674 $\pm$ 2.189	32.91 $\pm$ 11.21	0.0208 <sup>a</sup>
IL17	0.1038 $\pm$ 0.07858	0.4642 $\pm$ 0.3895	0.0173 <sup>a</sup>	0.4642 $\pm$ 0.3895	0.2036 $\pm$ 0.1209	0.4117

Note: Data are mean  $\pm$  SEM, P value was determined with Kruskal-Wallis test.

<sup>a</sup>Signifies statistical significance.

*Csf3r*<sup>+/+</sup> mice. We observed that the increased susceptibility of *Csf3r*<sup>-/-</sup> mice to acute colitis was associated with altered expression of inflammatory cytokines (Fig. 3B; Table 1), including decreased expression of IL22, as well as its upstream regulator IL23 (Fig. 3B–D; Table 1). IL22 is a pivotal cytokine for the maintenance and repair of the intestinal epithelium (25–28). Consistent with the decreased expression of IL22, which would be expected to lead to reduced IL22 activity (27), IHC analysis showed reduced STAT3 phosphorylation in colon tissue sections of DSS-treated *Csf3r*<sup>-/-</sup> mice, compared with DSS-treated *Csf3r*<sup>+/+</sup> mice (Fig. 3E and F).

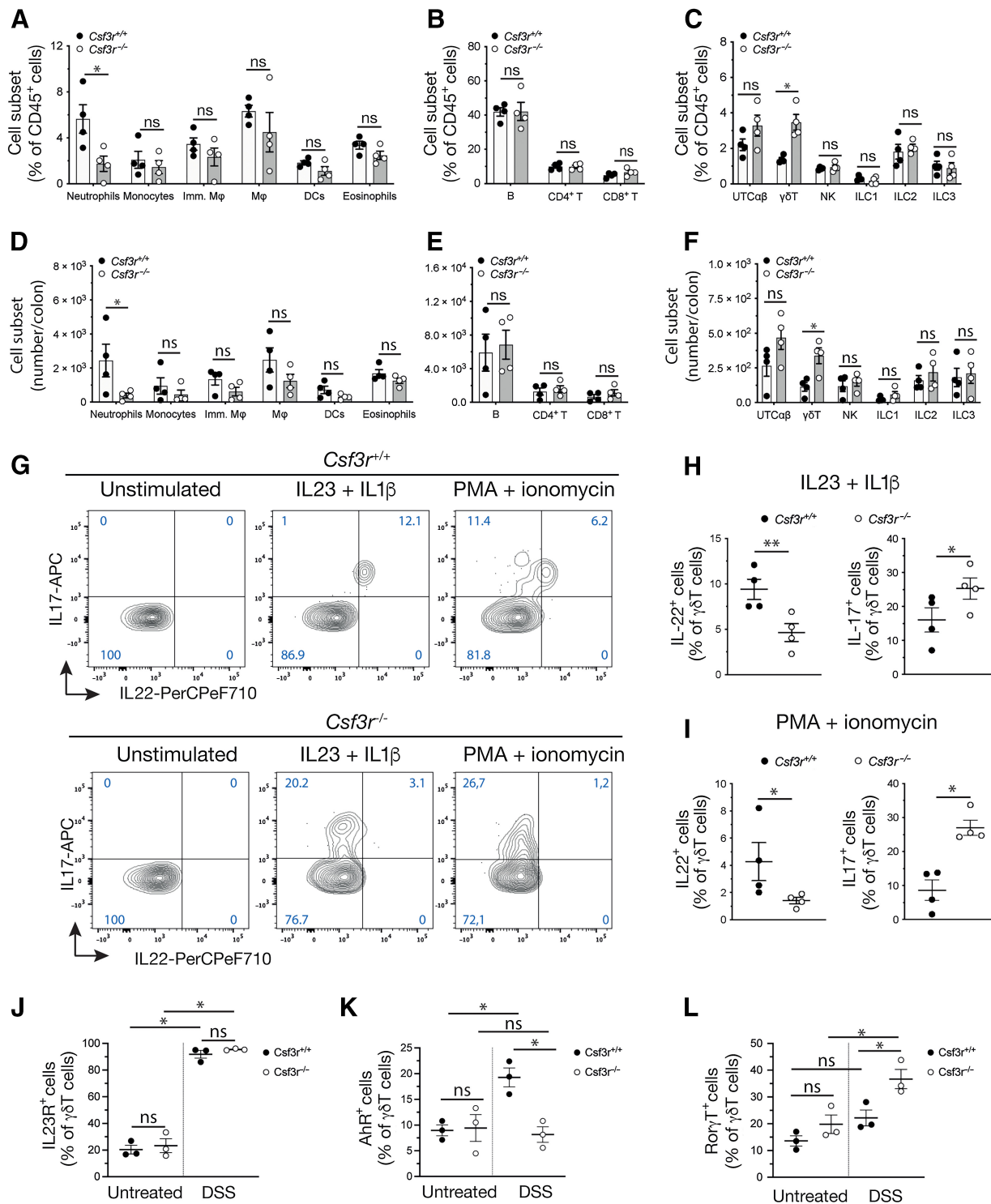
Neutrophil adoptive transfer in *Csf3r*<sup>-/-</sup> mice was sufficient to completely restore IL22 and IL23 tissue concentrations to the levels observed in *Csf3r*<sup>+/+</sup> mice (Fig. 3B–D and Table 1). Because IL23 is mostly produced by myeloid cells, in particular macrophages (37), we established an *in vitro* model to assess the impact of neutrophils on the production of IL23 by macrophages. Neutrophils did not produce IL23 but amplified IL23 expression by macrophages upon stimulation with GM-CSF and TLR9 agonist (Supplementary Fig. S3B). Under these conditions, we did not observe an increase in neutrophil apoptosis, ruling out an effect attributable to efferocytosis (Supplementary Fig. S3C). In contrast, the selective inhibition of ROS production in neutrophils or coculture of neutrophils and macrophages in transwell eliminated the contribution of neutrophils to IL23 production amplification (Supplementary Fig. S3B). Thus, neutrophils strengthened IL23 production in macrophages in a contact-dependent manner and through the release of ROS.

In line with the above findings, the adoptive transfer of naïve neutrophils in DSS-treated *Csf3r*<sup>-/-</sup> mice abolished the differences in the number of healing ulcers observed between *Csf3r*<sup>-/-</sup> and *Csf3r*<sup>+/+</sup> mice, and a complete re-epithelialization was observed in *Csf3r*<sup>-/-</sup> mice that underwent adoptive transfers of neutrophils (Fig. 3G). To underscore the *in vivo* relevance of the neutrophil–IL22 axis in colitis, we performed experiments in which the IL22 pathway was activated in *Csf3r*<sup>+/+</sup> and *Csf3r*<sup>-/-</sup> mice or blocked in *Csf3r*<sup>-/-</sup> mice that received neutrophil adoptive transfers. The administration of IL22 in DSS-treated *Csf3r*<sup>-/-</sup> mice significantly reduced the severity of colitis (Fig. 3H and I). These results support the hypothesis that the impaired production of IL22 observed in DSS-treated *Csf3r*<sup>-/-</sup> mice contributed to the increased pathological signs. Furthermore, *in vivo* neutralization of IL22 abolished the beneficial effect of the adoptive transfers of neutrophils observed in DSS-treated *Csf3r*<sup>-/-</sup> mice (Sup-

plementary Figs. S3D and S3E). Collectively, these results provide unequivocal evidence that neutrophils mediate protection against colitis by driving the formation of an IL22-dependent response.

#### The production of IL22 by $\gamma\delta$ T cells is impaired in neutrophil deficient mice

We characterized by flow cytometry the immune infiltrate in the colon lamina propria (LP) of *Csf3r*<sup>-/-</sup> and *Csf3r*<sup>+/+</sup> mice in the model of DSS-induced colitis. We observed that the number and frequency of neutrophils were significantly reduced in *Csf3r*<sup>-/-</sup> mice (Fig. 4A and D; Supplementary Fig. S4A). We did not observe any other significant differences in the immune infiltrate between *Csf3r*<sup>+/+</sup> and *Csf3r*<sup>-/-</sup> mice, except for a slight increase in the frequency and number of  $\gamma\delta$  T cells in *Csf3r*<sup>-/-</sup> mice (Fig. 4A–F; Supplementary Figs. S4A–S4D). To identify the cellular source of IL22 in the inflamed colon, total LPCs were stimulated *ex vivo* and further analyzed by intracellular cytokine staining (ICS). No differences were observed in myeloid cells (Supplementary Fig. S4E). Among analyzed lymphoid cells,  $\gamma\delta$  T cells were the most potent producers of IL22 (Supplementary Figs. S4F and S4G). In agreement with previous reports (38),  $\gamma\delta$  T cells from *Csf3r*<sup>+/+</sup> mice were polyfunctional and capable of simultaneously secreting IL22 and IL17 (Fig. 4G). Moreover, the activation state of  $\gamma\delta$  T cells from *Csf3r*<sup>-/-</sup> mice was altered towards decreased production of IL-22 and increased production of IL-17 (Fig. 4G–I). No differences were observed in CD4<sup>+</sup> T cells and in innate lymphoid cells (ILCs) (Supplementary Fig. S4F–S4G). Polarization and expression of IL-22 by  $\gamma\delta$  T cells depend on different factors, including expression of IL-23 receptor (IL-23R) and aryl hydrocarbon receptor (AhR) (26, 39, 40). We better characterized the features of colonic LP  $\gamma\delta$  T cells of untreated and DSS-treated mice by flow cytometry. We found similar expression levels of IL-23R, AhR, and ROR $\gamma$ t in  $\gamma\delta$  T cells from untreated *Csf3r*<sup>+/+</sup> and *Csf3r*<sup>-/-</sup> mice (Fig. 4J–L). However, while the expression of IL-23R in  $\gamma\delta$  T cells of both genotypes was similar in DSS-treated mice,  $\gamma\delta$  T cells of DSS-treated *Csf3r*<sup>-/-</sup> mice showed increased expression of ROR $\gamma$ t and reduced expression of AhR (Fig. 4J–L). Distinct subsets of  $\gamma\delta$  T cells with variable capacities to produce cytokines have been defined according to their expression of CD27 (38, 41). We did not find any differences in the frequencies of CD27<sup>+</sup> ( $\gamma\delta$ 27<sup>+</sup>) or CD27<sup>-</sup> ( $\gamma\delta$ 27<sup>-</sup>)  $\gamma\delta$  T-cell subsets in the colon LP of DSS-treated *Csf3r*<sup>-/-</sup> and *Csf3r*<sup>+/+</sup> mice (Supplementary Fig. S5A and S5B). However,  $\gamma\delta$ 27<sup>-</sup> cells from DSS-treated *Csf3r*<sup>-/-</sup> mice showed

**Figure 4.**

Neutrophil deficiency is associated with impaired polarization and production of IL22 by  $\gamma\delta$  T cells. **A–F**, Quantification of immune cell subset frequencies (**A–C**) and numbers (**D–F**) in colon LP of DSS-treated *Csf3r*<sup>+/+</sup> ( $n = 4$ ) and *Csf3r*<sup>-/-</sup> ( $n = 4$ ) mice. UTC, unconventional T cells (TCR $\beta$ <sup>+</sup>, CD8<sup>-</sup>, CD4<sup>-</sup>). **G**, Representative dot-plot of IL22 and IL17 flow cytometry analysis in  $\gamma\delta$  T cells from unstimulated, IL23 plus IL1 $\beta$ , and PMA plus ionomycin stimulated LPCs derived from DSS-treated *Csf3r*<sup>+/+</sup> (top) and *Csf3r*<sup>-/-</sup> (bottom) mice. **H** and **I**, Expression of IL22 (left) and IL17 (right) by  $\gamma\delta$  T cells stimulated 4 hours with IL23 plus IL1 $\beta$  (**H**) and PMA plus ionomycin (**I**) analyzed by flow cytometry (*Csf3r*<sup>+/+</sup>  $n = 4$ , *Csf3r*<sup>-/-</sup>  $n = 4$ ). **J–L**, Expression of IL-23R (**J**), AhR (**K**), and Ror $\gamma$ T (**L**) in  $\gamma\delta$  T cells from colon LP of untreated and DSS-treated *Csf3r*<sup>+/+</sup> ( $n = 3$ ) and *Csf3r*<sup>-/-</sup> ( $n = 3$ ) mice analyzed by flow cytometry. **A–J**, Representative data of three independent experiments. **A–F**, Multiple  $t$  test. **H–L**, Unpaired Student  $t$  test. Data are mean  $\pm$  SEM. \*,  $P < 0.05$ ; \*\*,  $P < 0.01$ ; \*\*\*,  $P < 0.001$ ; ns, not significant.



decreased expression of AhR and IL-22 associated with increased expression of ROR $\gamma$ t and IL-17 (Supplementary Fig. S5C–S5H). As observed in previous reports (38),  $\gamma\delta$ 27 $^{+}$  cells from *Csf3r* $^{+/+}$  mice expressed IL-22 and IL-17 whereas the expression of these cytokines was almost undetectable in  $\gamma\delta$ 27 $^{+}$  cells (Supplementary Fig. S5D–S5G). Collectively, these data show that neutrophil deficiency was associated with altered polarization of  $\gamma\delta$ 27 $^{+}$  cells toward decreased expression of AhR and IL-22.

### Cross-talk between neutrophils and $\gamma\delta$ T cells mediates protection in colitis

Having established that neutrophils played a key role in the polarization of  $\gamma\delta$  T cells toward IL22 production, it was important

to evaluate the *in vivo* impact of the neutrophil– $\gamma\delta$  T-cell axis in colitis. We found that the lack of  $\gamma\delta$  T cells in *Tcrd* $^{-/-}$  mice was associated with increased susceptibility to DSS-induced colitis compared with wild-type mice, as reported previously (Fig. 5A; ref. 42). Adoptive transfers of neutrophils had no effect on the severity of colitis observed in *Tcrd* $^{-/-}$  mice, demonstrating that  $\gamma\delta$  T cells were required for the beneficial effect of neutrophils (Fig. 5A).

Given that our data showed that intestinal dysbiosis observed in *Csf3r* $^{-/-}$  mice was associated with increased susceptibility to colitis, we evaluated the impact of microbiota and neutrophils directly on polarization and IL22 production by  $\gamma\delta$  T cells. We treated *Csf3r* $^{+/+}$ , *Csf3r* $^{-/-}$ , and *Csf3r* $^{-/-}$  mice receiving adoptive transfers of neutrophils with or without broad spectrum ABX and challenged the mice

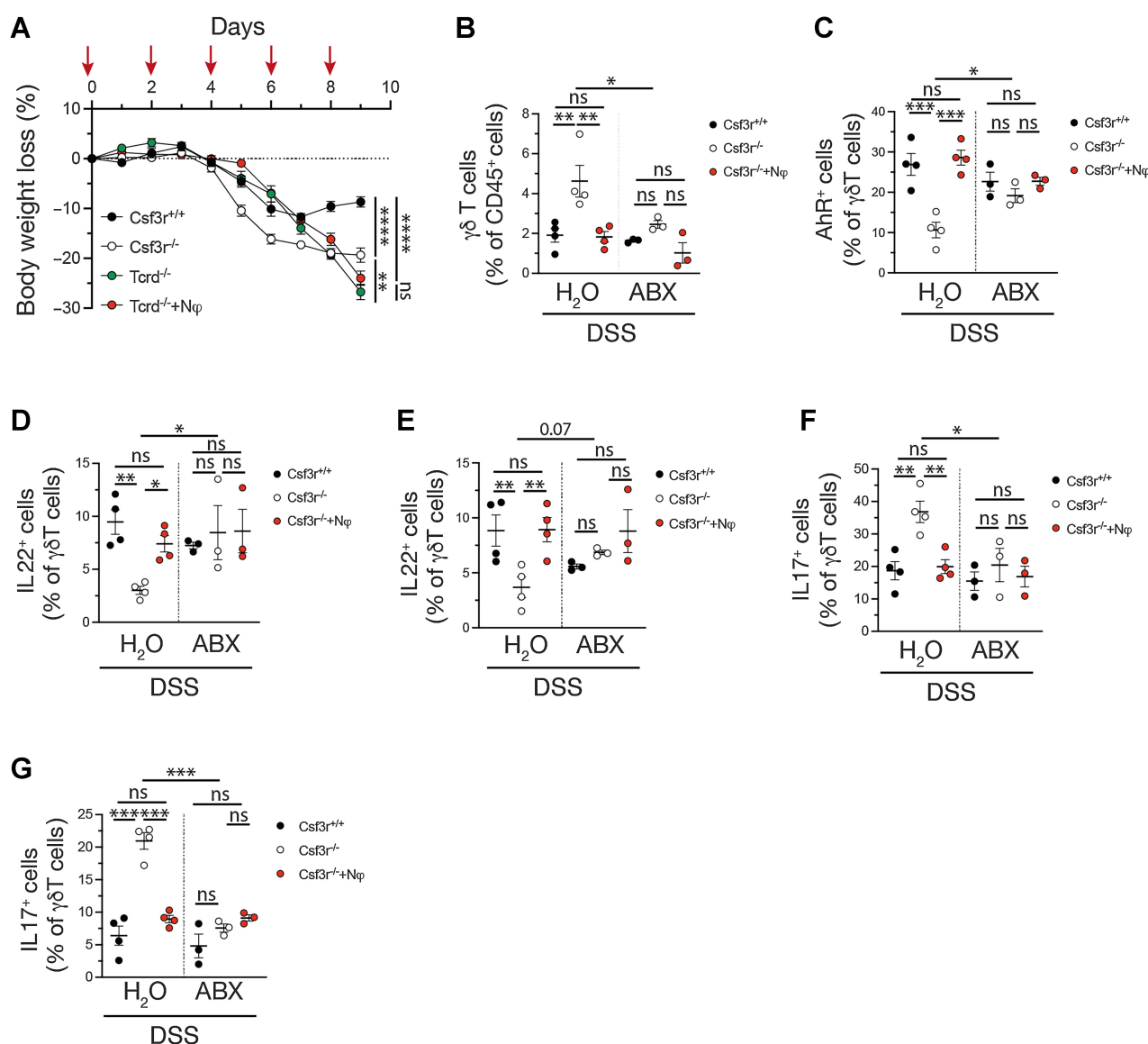


**Figure 5.**

Neutrophils regulate  $\gamma\delta$  T cells polarization through the control of the intestinal microbiota. **A**, Body weight loss during DSS-induced acute colitis in *Csf3r* $^{+/+}$  ( $n = 4$ ), *Csf3r* $^{-/-}$  ( $n = 4$ ), *Tcrd* $^{-/-}$  ( $n = 4$ ), and *Tcrd* $^{-/-}$  mice upon adoptive transfer of neutrophils (N $\phi$ ;  $n = 4$ ). Red arrows indicated days of neutrophils transfer. **B**, Frequency of  $\gamma\delta$  T cells from colon LP of DSS-treated mice. **C**, AhR expression in  $\gamma\delta$  T cells from colon LP of DSS-treated mice. **D** and **E**, Expression of IL22 by  $\gamma\delta$  T cells stimulated 4 hours with IL23 plus IL1 $\beta$  (**D**) and PMA plus ionomycin (**E**) analyzed by flow cytometry. **F** and **G**, Expression of IL17 by  $\gamma\delta$  T cells stimulated 4 hours with IL23 plus IL1 $\beta$  (**F**) and PMA plus ionomycin (**G**) analyzed by flow cytometry. **A**, Representative data of two independent experiments. **B–G**, One experiment (*Csf3r* $^{+/+}$   $n = 4$ , *Csf3r* $^{-/-}$ +ABX  $n = 3$ , *Csf3r* $^{-/-}$   $n = 4$ , and *Csf3r* $^{-/-}$ +ABX  $n = 3$ , *Csf3r* $^{-/-}$ +N $\phi$   $n = 4$ , *Csf3r* $^{-/-}$ +N $\phi$ +ABX  $n = 3$ ). **A**, Wilcoxon matched-pairs signed rank test. **B–G**, One-way ANOVA. Data are mean  $\pm$  SEM. \*,  $P < 0.05$ ; \*\*,  $P < 0.01$ ; \*\*\*,  $P < 0.001$ ; ns, not significant.

with the model of DSS-induced colitis (Supplementary Fig. S5I). Both adoptive transfer of neutrophils and ABX treatment were sufficient to reduce colitis severity and the frequency of  $\gamma\delta$  T cells in colon LP of DSS-treated *Csf3r*<sup>-/-</sup> mice (Fig. 5B; Supplementary Fig. S5I). In addition, these treatments were also sufficient to rescue the polarization and activation state of  $\gamma\delta$  T cells toward high expression of AhR and IL22 and low expression of IL17 (Fig. 5B–G). The adoptive transfer of neutrophils was ineffective in modifying the expression of AhR, IL22, and IL17 in  $\gamma\delta$  T cells from *Csf3r*<sup>-/-</sup> mice receiving ABX treatment. Therefore, these data supported a model in which neutrophils controlling the intestinal microbiota were essential for  $\gamma\delta$  T-cell polarization and IL22 production.

### Neutrophil infiltration is associated with the expression of IL22, IL23, and tissue repair gene signatures in patients with ulcerative colitis

To assess the relevance of our mouse model data to humans, we analyzed public datasets of RNA sequencing of rectal biopsies from treatment-naïve patients [pediatric patients (GSE109142) and adult patients (GSE87473)] with UC. In both, *CSF3R* expression was positively associated with *IL23*, *IL22*, and *AHR* expression (Fig. 6A–F). In addition, by stratifying patients according to *CSF3R* expression levels and performing GSEA, we detected a significant enrichment of gene signatures associated with epithelial cell development and proliferation, and antimicrobial activity in *CSF3R*<sup>high</sup> UC patients

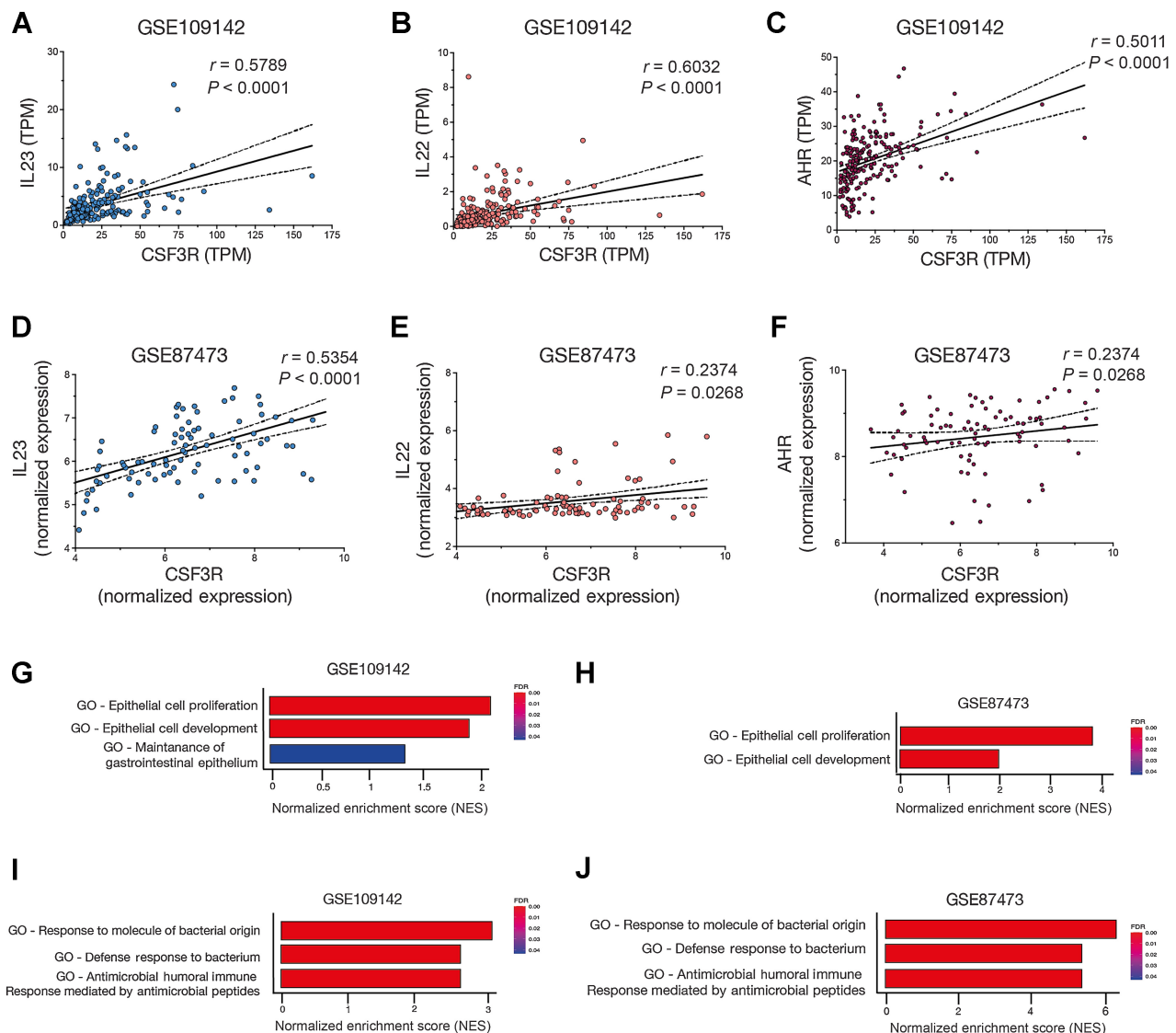


**Figure 6.**

Neutrophil infiltration is associated with tissue repair gene signatures in patients with ulcerative colitis. **A–F**, Spearman correlation between *CSF3R* and *IL23* expression (**A–D**), *CSF3R* and *IL22* expression (**B–E**), and *CSF3R* and *AHR* (**C–F**) in UC patients GSE109142 (pediatric patients,  $n = 206$ ) and GSE87473 (adult patients,  $n = 87$ ). **G** and **H**, Bar plot representing GSEA for epithelial GO signatures in *CSF3R*<sup>high</sup> versus *CSF3R*<sup>low</sup> UC patients GSE109142 (**E**) and GSE87473 (**F**). **I** and **J**, Bar plot representing GSEA for antimicrobial response GO signatures in *CSF3R*<sup>high</sup> versus *CSF3R*<sup>low</sup> UC patients from the dataset GSE109142 (**I**) and GSE87473 (**J**). *CSF3R* gene expression values were stratified by quartiles and patients belonging to the upper (GSE109142,  $n = 51$ ; GSE87473,  $n = 21$ ) and lower GSE109142,  $n = 51$ ; GSE87473,  $n = 21$ ) quartiles were considered for differential expression analysis.



(Fig. 6G–J; Supplementary Fig. S6). Collectively, these results suggest that like the findings in DSS-induced colitis in mice, a neutrophil–IL22 axis may be involved in tissue repair and control of intestinal microbiota in human UC.

## Discussion

The existence of a link between inflammation and cancer has long been established (43). In particular, the association between intestinal inflammation and the development of colorectal cancer has served as a paradigm to study the role of inflammation in cancer (5–8). Neutrophils have been proposed to play a role in UC and in colorectal cancer, including in CAC (12–21, 44). However, results reported in the literature have described both beneficial and detrimental roles for neutrophils. Here, we provided genetic evidence based on *Csf3r*<sup>−/−</sup> mice, supported by adoptive cell transfer experiments and analysis of human datasets, that neutrophils are essential to limit intestinal inflammation, bacterial infiltration, and the development of CAC. We showed that the protection was associated with control of the intestinal microbiota and the promotion of the expression of IL22, which is known to support mucosal healing and repair of the intestinal epithelial barrier and genome integrity of intestinal epithelial stem cells (26–28, 45). The latter is important since tissue repair of damaged intestinal epithelial barrier prevents the infiltration of microbes that could act as an amplifier of detrimental inflammation (46, 47).

Our observations showed that neutrophil deficiency determines increased susceptibility to DSS-induced colitis and AOM/DSS-induced CAC, as evidenced by increased body weight loss, colitis grade, and polyp number in *Csf3r*<sup>−/−</sup> mice, compared with *Csf3r*<sup>+/+</sup> mice. The adoptive transfer of neutrophils was sufficient to reduce the severity of colitis in *Csf3r*<sup>−/−</sup> mice, underlining their protective role during intestinal inflammation.

Microbiota dysregulation has long been associated with IBD and colorectal cancer (11, 48–50). Interestingly, neutrophils have recently been implicated in the control of intestinal microbiota (12, 14). Our results indicate that neutrophil deficiency determined increased bacterial infiltration into the ulcerated intestinal mucosa. Consistent with this, a metagenomic analysis revealed that *Csf3r*<sup>−/−</sup> mice displayed alterations in the microbiota composition both at steady-state and during inflammation. We observed an increased frequency of *Actinobacteria* in untreated *Csf3r*<sup>−/−</sup> and three *phyla* were almost exclusively present in *Csf3r*<sup>−/−</sup> mice (i.e., *Actinobacteria*, *Tenericutes*, and *Patescibacteria*). Interestingly, the increased frequency of *Actinobacteria* has been associated with IBD in humans (51, 52). The pathological role of altered intestinal microbiota in *Csf3r*<sup>−/−</sup> mice was further demonstrated by broad-spectrum antibiotic treatment and cohousing experiments of *Csf3r*<sup>−/−</sup> with *Csf3r*<sup>+/+</sup> mice, which dramatically reduced the severity of colitis and CAC in *Csf3r*<sup>−/−</sup> mice. Altogether, these results indicate that neutrophils play an important role in controlling the intestinal microbiota, which is known to play an important role in the development of intestinal inflammation and CAC (11, 48–50).

Histopathologic analysis of colon specimens from DSS-treated mice showed a defect in epithelial regeneration in *Csf3r*<sup>−/−</sup> mice, demonstrated by a reduction in the number of healing ulcers. This phenotype is rescued by the adoptive transfer of neutrophils, indicating the involvement of neutrophils in the process of tissue repair. IL22/p-STAT3 axis is a critical signaling pathway that drives mucosal healing and repair of the intestinal epithelial barrier (27, 28). Interestingly, IL22 levels in colon specimens from DSS-treated mice were reduced in *Csf3r*<sup>−/−</sup> mice compared with *Csf3r*<sup>+/+</sup> mice. Consistent with the

lower levels of IL22 in neutrophil deficient mice, pSTAT3 expression on tissue sections was also reduced in *Csf3r*<sup>−/−</sup> mice. The treatment of DSS-treated *Csf3r*<sup>−/−</sup> mice with IL22 was sufficient to reduce their pathologic signs to the level observed in DSS-treated *Csf3r*<sup>+/+</sup> mice. Moreover, neutrophil adoptive transfer restored the expression of IL22 in DSS-treated *Csf3r*<sup>−/−</sup> mice and the blockade of IL22 abolished the beneficial effect of the adoptive transfer, demonstrating the importance of neutrophils in the formation of an IL22-dependent intestinal reparative response. In addition to IL22, levels of other cytokines in colon tissue were also altered in DSS-treated *Csf3r*<sup>−/−</sup> mice compared with DSS-treated *Csf3r*<sup>+/+</sup> mice. In particular, we observed decreased levels of IL10 and elevated levels of IL17, which represent phenotypes previously associated with increased susceptibility to colitis (14, 53). Of note, we did not observe any alteration in the presence of Foxp3<sup>+</sup> CD4<sup>+</sup> regulatory T cells in the colon LP of DSS-treated *Csf3r*<sup>−/−</sup> mice. Although our results did not exclude that these alterations could play a role in the observed phenotype, our findings unequivocally demonstrate the contribution of the protective neutrophil–IL22 axis.

To address the cellular sources of IL22, we performed flow cytometry analysis of LP cells. Previous work reported the production of IL22 by neutrophils (54). However, we found that only a very low percentage of stimulated neutrophils produced IL22, suggesting that neutrophils were not a major source of IL22. Other myeloid cells also produced low amounts of IL-22 and their capacity to produce IL22 in response to cytokine stimulation was not affected in *Csf3r*<sup>−/−</sup> cells. Among lymphoid cells, only  $\gamma\delta$  T cells derived from *Csf3r*<sup>−/−</sup> mice displayed a reduced capacity to produce IL22 in response to *ex vivo* stimulation. In particular, we found decreased expression of IL22 in  $\gamma\delta 27^{-}$  cells, while the frequency of  $\gamma\delta 27^{-}$  and  $\gamma\delta 27^{+}$  in colon LP was unaltered between *Csf3r*<sup>+/+</sup> and *Csf3r*<sup>−/−</sup> mice. ILC3s have been shown to represent an important source of IL22 in the intestine (26, 55), however, our data did not show any alteration in the frequency or capacity to produce IL22 in ILC3s derived from DSS-treated wild-type or *Csf3r*<sup>−/−</sup> mice.

The production of IL22 by lymphoid cells, including  $\gamma\delta$  T cells, is dependent on environmental factors, such as the expression of IL23 by myeloid cells, and it requires the engagement of AhR (39, 40). In turn, the expression of AhR by  $\gamma\delta$  T cells is enhanced by IL23 and IL1 $\beta$ , and by food- and bacteria-derived metabolites (26, 39, 40, 56, 57). We found reduced levels of IL23 and IL1 $\beta$  in colon specimens derived from DSS-treated *Csf3r*<sup>−/−</sup> mice associated with decreased expression of AhR in *Csf3r*<sup>−/−</sup>  $\gamma\delta$  T cells, indicating a defect in the upstream regulation of IL22 production in *Csf3r*<sup>−/−</sup> mice. Mechanistically, we showed that neutrophils amplified the expression of IL23 by macrophages stimulated with a TLR9 agonist in a contact-dependent manner and through the release of ROS. These results suggest that neutrophils support the production of IL23 in myeloid cells and, in turn, the expression of IL22 in  $\gamma\delta$  T cells. Others have suggested that the phenotype and functional characteristics of  $\gamma\delta$  T cells can be shaped by microbiota in other contexts (58, 59). In line with this hypothesis, we found that the impaired polarization and IL22 production of  $\gamma\delta$  T cells from *Csf3r*<sup>−/−</sup> mice can be restored by neutrophil adoptive transfer or antibiotic treatment, defining a model in which neutrophils, through the control of microbiota and inflammatory response, shape the polarization of  $\gamma\delta$  T cells toward high expression of AhR and IL22. Importantly, neutrophil adoptive transfer was not sufficient to reduce colitis severity in *Tcrd*<sup>−/−</sup> mice, indicating that the cross-talk between neutrophils and  $\gamma\delta$  T cells was essential to mount a protective response against colitis. Collectively, these results highlighted the pivotal role played by neutrophils in the establishment of a protective pathway

against colitis, which is necessary to prevent inflammation and subsequent carcinogenesis.

Further analysis showed that *CSF3R* expression is positively correlated with *IL23*, *IL22*, and *AHR* expression in UC patients, indicating an association between neutrophils and the IL22-dependent protective axis in humans. Indeed, IL22 expression has been associated with mucosal healing in human UC and administration of IL22 in patients with UC is being tested in clinical trials (46). Moreover, patient stratification according to *CSF3R* expression showed the enrichment of epithelial repair and regeneration gene signatures in *CSF3R*<sup>high</sup> patients in two independent datasets of UC patients.

The findings reported here highlight the importance of neutrophils in maintaining intestinal homeostasis in response to inflammatory insults and describe a model where neutrophils control the susceptibility to intestinal inflammation and CAC by shaping the intestinal microbiota composition and the activation of an IL22-dependent tissue repair pathway (Supplementary Fig. S7).

### Authors' Disclosures

C. Garlanda reports grants from Ministero della Salute during the conduct of the study. A. Mantovani reports personal fees from Ventana, Pierre Fabre, Verily, Abbvie, Astra Zeneca, Verseau Therapeutics, Myeloid Therapeutics, Third Rock Venture, Imcheck Therapeutics, Ellipses, Novartis, Roche, Macrophage Pharma, Biovelocita, Merck, Principia, Biolegend, Olatec Therapeutics, Moderna, and Henlius outside the submitted work, grants from Novartis, other support from Cedarlane, HyCult, eBioscience, Biolegend, ABCAM, Novus Biologicals, Enzo Life, Affymetrix, and also has a patent for WO2019057780 "Anti-human migration stimulating factor (MSF) and uses thereof" pending and issued, a patent for WO2019081591 "NK or T cells and uses thereof" pending and issued, a patent for WO2020127471 "Use of SAP for the treatment of Eumycetes fungi infections" pending and issued, and a patent for EP20182181.6 "PTX3 as prognostic marker in Covid-19" pending and licensed to Diasorin. S. Jaillon reports grants from Italian Ministry of Health, Italian Association for Cancer Research AIRC, and Italian Ministry of University and Research during the conduct of the study. No disclosures were reported by the other authors.

### References

- Borregaard N. Neutrophils, from marrow to microbes. *Immunity* 2010;33:657–70.
- Mantovani A, Cassatella MA, Costantini C, Jaillon S. Neutrophils in the activation and regulation of innate and adaptive immunity. *Nat Rev Immunol* 2011;11:519–31.
- Jaillon S, Ponzetta A, Di Mitri D, Santoni A, Bonocchi R, Mantovani A. Neutrophil diversity and plasticity in tumour progression and therapy. *Nat Rev Cancer* 2020;20:485–503.
- Sung H, Ferlay J, Siegel RL, Laversanne M, Soerjomataram I, Jemal A, et al. Global cancer statistics 2020: GLOBOCAN estimates of incidence and mortality worldwide for 36 cancers in 185 countries. *CA Cancer J Clin* 2021;71:209–49.
- Eaden JA, Abrams KR, Mayberry JF. The risk of colorectal cancer in ulcerative colitis: a meta-analysis. *Gut* 2001;48:526–35.
- Jess T, Rungoe C, Peyrin-Biroulet L. Risk of colorectal cancer in patients with ulcerative colitis: a meta-analysis of population-based cohort studies. *Clin Gastroenterol Hepatol* 2012;10:639–45.
- Fumery M, Dulai PS, Gupta S, Prokop LJ, Ramamoorthy S, Sandborn WJ, et al. Incidence, risk factors, and outcomes of colorectal cancer in patients with ulcerative colitis with low-grade dysplasia: a systematic review and meta-analysis. *Clin Gastroenterol Hepatol* 2017;15:665–74.
- Olen O, Erichsen R, Sachs MC, Pedersen L, Halfvarson J, Askling J, et al. Colorectal cancer in ulcerative colitis: a Scandinavian population-based cohort study. *Lancet* 2020;395:123–31.
- Grivennikov SI. Inflammation and colorectal cancer: colitis-associated neoplasia. *Semin Immunopathol* 2013;35:229–44.
- Shah SC, Itzkowitz SH. Colorectal cancer in inflammatory bowel disease: mechanisms and management. *Gastroenterology* 2022;162:715–30.
- Park EM, Chelvanambi M, Bhutiani N, Kroemer G, Zitvogel L, Wargo JA. Targeting the gut and tumor microbiota in cancer. *Nat Med* 2022;28:690–703.
- Dmitrieva-Posocco O, Dzutsev A, Posocco DF, Hou V, Yuan W, Thovarai V, et al. Cell-type-specific responses to interleukin-1 control microbial invasion and tumor-elicited inflammation in colorectal cancer. *Immunity* 2019;50:166–80.
- Li Y, Zhu L, Chu Z, Yang T, Sun HX, Yang F, et al. Characterization and biological significance of IL-23-induced neutrophil polarization. *Cell Mol Immunol* 2018;15:518–30.
- Triner D, Devenport SN, Ramakrishnan SK, Ma X, Frieler RA, Greenon JK, et al. Neutrophils restrict tumor-associated microbiota to reduce growth and invasion of colon tumors in mice. *Gastroenterology* 2019;156:1467–82.
- Leppkes M, Lindemann A, Gosswein S, Paulus S, Roth D, Hartung A, et al. Neutrophils prevent rectal bleeding in ulcerative colitis by peptidyl-arginine deiminase-4-dependent immunothrombosis. *Gut* 2022;71:2414–29.
- Wang X, Cai J, Lin B, Ma M, Tao Y, Zhou Y, et al. GPR34-mediated sensing of lysophosphatidylserine released by apoptotic neutrophils activates type 3 innate lymphoid cells to mediate tissue repair. *Immunity* 2021;54:1123–36.
- Wang Y, Wang K, Han GC, Wang RX, Xiao H, Hou CM, et al. Neutrophil infiltration favors colitis-associated tumorigenesis by activating the interleukin-1 (IL-1)/IL-6 axis. *Mucosal Immunol* 2014;7:1106–15.
- Zhou G, Yu L, Fang L, Yang W, Yu T, Miao Y, et al. CD177(+) neutrophils as functionally activated neutrophils negatively regulate IBD. *Gut* 2018;67:1052–63.
- Pavlidis P, Tsakmaki A, Pantazi E, Li K, Cozzetto D, Digby-Bell J, et al. Interleukin-22 regulates neutrophil recruitment in ulcerative colitis and is associated with resistance to ustekinumab therapy. *Nat Commun* 2022;13:5820.
- Salas A. What good can neutrophils do in UC? *Gut* 2022;71:2375–6.

### Authors' Contributions

S. Carnevale: Formal analysis, investigation, methodology, writing—original draft, writing—review and editing. A. Ponzetta: Formal analysis, investigation, methodology, writing—original draft, writing—review and editing. A. Rigatelli: Formal analysis, investigation, methodology. R. Carriero: Formal analysis, investigation, methodology. S. Puccio: Formal analysis, investigation, methodology. D. Supino: Investigation, methodology. G. Grieco: Investigation, methodology. P. Molisso: Investigation, methodology. I. Di Ceglie: Investigation, methodology. F. Scavella: Investigation, methodology. C. Perucchini: Methodology. F. Pasqualini: Methodology. C. Recordati: Methodology. C. Tripodo: Funding acquisition, methodology. B. Belmonte: Methodology. A. Mariancini: Methodology. P. Kunderfranco: Formal analysis, methodology. G. Sciumè: Methodology, writing—review and editing. E. Lugli: Methodology, writing—review and editing. E. Bonavita: Methodology, writing—review and editing. E. Magrini: Methodology, writing—review and editing. C. Garlanda: Funding acquisition, writing—review and editing. A. Mantovani: Funding acquisition, writing—review and editing. S. Jaillon: Conceptualization, supervision, funding acquisition, writing—original draft, writing—review and editing.

### Acknowledgments

This research was funded by Italian Ministry of Health-GR-2016-02361263 to S. Jaillon, the European Union - Next Generation EU - NRRP M6C2 - Investment 2.1 Enhancement and strengthening of biomedical research in the NHS - PNRR-MAD-2022-12375947 to C. Garlanda and S. Jaillon, the Italian Association for Cancer Research AIRC IG-22815 to S. Jaillon and IG-23465 to A. Mantovani, and Italian Ministry of University and Research - PRIN 2017K7FSYB to S. Jaillon and C. Tripodo. S. Carnevale and S. Puccio are recipients of a fellowship from the Italian Association for Cancer Research. E. Lugli is a CRI Lloyd J. Old STAR (CRI Award 3914). The purchase of a FACSymphony A5 was defrayed in part by a grant from the Italian Ministry of Health (agreement 82/2015). We thank Dr. Gabriele De Simone and Dr. Chiara Camisaschi from the Humanitas Flow Cytometry Core Facility for cell sorting experiments.

### Note

Supplementary data for this article are available at Cancer Immunology Research Online (<http://cancerimmunolres.aacrjournals.org/>).

Received April 7, 2023; revised December 1, 2023; accepted February 9, 2024; published first February 13, 2024.

21. Broggi A, Tan Y, Granucci F, Zanoni I. IFN-lambda suppresses intestinal inflammation by non-translational regulation of neutrophil function. *Nat Immunol* 2017;18:1084–93.
22. Ponzetta A, Carriero R, Carnevale S, Barbagallo M, Molgora M, Perucchini C, et al. Neutrophils driving unconventional T cells mediate resistance against murine sarcomas and selected human tumors. *Cell* 2019;178:346–60.
23. Garlanda C, Riva F, Veliz T, Polentarutti N, Pasqualini F, Radaelli E, et al. Increased susceptibility to colitis-associated cancer of mice lacking TIR8, an inhibitory member of the interleukin-1 receptor family. *Cancer Res* 2007;67:6017–21.
24. Eichele DD, Kharbanda KK. Dextran sodium sulfate colitis murine model: An indispensable tool for advancing our understanding of inflammatory bowel diseases pathogenesis. *World J Gastroenterol* 2017;23:6016–29.
25. Fakhrullina AR, Peshkova IO, Dzutsev A, Aghayev T, McCulloch JA, Thovara V, et al. An interleukin-23-interleukin-22 axis regulates intestinal microbial homeostasis to protect from diet-induced atherosclerosis. *Immunity* 2018;49:943–57.
26. Gronke K, Hernandez PP, Zimmermann J, Klose CSN, Kofoed-Branzk M, Guendel F, et al. Interleukin-22 protects intestinal stem cells against genotoxic stress. *Nature* 2019;566:249–53.
27. Pickert G, Neufert C, Leppkes M, Zheng Y, Wittkopf N, Warntjen M, et al. STAT3 links IL-22 signaling in intestinal epithelial cells to mucosal wound healing. *J Exp Med* 2009;206:1465–72.
28. Wolk K, Kunz S, Witte E, Friedrich M, Asadullah K, Sabat R. IL-22 increases the innate immunity of tissues. *Immunity* 2004;21:241–54.
29. Ballesteros I, Rubio-Ponce A, Genua M, Lusito E, Kwok I, Fernandez-Calvo G, et al. Co-option of neutrophil fates by tissue environments. *Cell* 2020;183:1282–97.
30. Caruso R, Ono M, Bunker ME, Nunez G, Inohara N. Dynamic and asymmetric changes of the microbial communities after cohousing in laboratory mice. *Cell Rep* 2019;27:3401–12.
31. Molgora M, Bonavita E, Ponzetta A, Riva F, Barbagallo M, Jaillon S, et al. IL-1R8 is a checkpoint in NK cells regulating anti-tumour and anti-viral activity. *Nature* 2017;551:110–4.
32. Quast C, Priesse E, Yilmaz P, Gerken J, Schweer T, Yarza P, et al. The SILVA ribosomal RNA gene database project: improved data processing and web-based tools. *Nucleic Acids Res* 2013;41(Database issue):D590–6.
33. Brummelman J, Haftmann C, Nunez NG, Alvisi G, Mazza EMC, Becher B, et al. Development, application and computational analysis of high-dimensional fluorescent antibody panels for single-cell flow cytometry. *Nat Protoc* 2019;14:1946–69.
34. Kranich J, Krautler NJ, Heinen E, Polymenidou M, Bridel C, Schildknecht A, et al. Follicular dendritic cells control engulfment of apoptotic bodies by secreting Mfge8. *J Exp Med* 2008;205:1293–302.
35. Moore RJ, Stanley D. Experimental design considerations in microbiota/inflammation studies. *Clin Transl Immunology* 2016;5:e92.
36. Karin M, Clevers H. Reparative inflammation takes charge of tissue regeneration. *Nature* 2016;529:307–15.
37. Maloy KJ, Powrie F. Intestinal homeostasis and its breakdown in inflammatory bowel disease. *Nature* 2011;474:298–306.
38. Barros-Martins J, Schmolka N, Fontinha D, Pires de Miranda M, Simas JP, Brok I, et al. Effector gammadelta T cell differentiation relies on master but not auxiliary th cell transcription factors. *J Immunol* 2016;196:3642–52.
39. Ness-Schwickerath KJ, Morita CT. Regulation and function of IL-17A- and IL-22-producing gammadelta T cells. *Cell Mol Life Sci* 2011;68:2371–90.
40. Martin B, Hirota K, Cua DJ, Stockinger B, Veldhoen M. Interleukin-17-producing gammadelta T cells selectively expand in response to pathogen products and environmental signals. *Immunity* 2009;31:321–30.
41. Ribot JC, deBarros A, Pang DJ, Neves JF, Peperzak V, Roberts SJ, et al. CD27 is a thymic determinant of the balance between interferon-gamma- and interleukin 17-producing gammadelta T cell subsets. *Nat Immunol* 2009;10:427–36.
42. Chen Y, Chou K, Fuchs E, Havran WL, Boismenu R. Protection of the intestinal mucosa by intraepithelial gamma delta T cells. *Proc Natl Acad Sci USA* 2002;99:14338–43.
43. Mantovani A, Allavena P, Sica A, Balkwill F. Cancer-related inflammation. *Nature* 2008;454:436–44.
44. Tosti N, Cremonesi E, Governa V, Basso C, Kancherla V, Coto-Llerena M, et al. Infiltration by IL22-producing T cells promotes neutrophil recruitment and predicts favorable clinical outcome in human colorectal cancer. *Cancer Immunol Res* 2020;8:1452–62.
45. Lindemans CA, Calafiore M, Mertelsmann AM, O'Connor MH, Dudakov JA, Jenq RR, et al. Interleukin-22 promotes intestinal-stem-cell-mediated epithelial regeneration. *Nature* 2015;528:560–4.
46. Keir M, Yi Y, Lu T, Ghilardi N. The role of IL-22 in intestinal health and disease. *J Exp Med* 2020;217:e20192195.
47. Mizoguchi A, Yano A, Himuro H, Ezaki Y, Sadanaga T, Mizoguchi E. Clinical importance of IL-22 cascade in IBD. *J Gastroenterol* 2018;53:465–74.
48. Belkaid Y, Hand TW. Role of the microbiota in immunity and inflammation. *Cell* 2014;157:121–41.
49. McQuade JL, Daniel CR, Helmink BA, Wargo JA. Modulating the microbiome to improve therapeutic response in cancer. *Lancet Oncol* 2019;20:e77–91.
50. Zagato E, Pozzi C, Bertocchi A, Schioppa T, Saccheri F, Guglietta S, et al. Endogenous murine microbiota member *Faecalibaculum rodentium* and its human homologue protect from intestinal tumour growth. *Nat Microbiol* 2020;5:511–24.
51. Barberio B, Facchin S, Patuzzi I, Ford AC, Massimi D, Valle G, et al. A specific microbiota signature is associated to various degrees of ulcerative colitis as assessed by a machine learning approach. *Gut Microbes* 2022;14:2028366.
52. Alam MT, Amos GCA, Murphy ARJ, Murch S, Wellington EMH, Arasaradnam RP. Microbial imbalance in inflammatory bowel disease patients at different taxonomic levels. *Gut Pathog* 2020;12:1.
53. Berg DJ, Zhang J, Weinstock JV, Ismail HF, Earle KA, Alila H, et al. Rapid development of colitis in NSAID-treated IL-10-deficient mice. *Gastroenterology* 2002;123:1527–42.
54. Zindl CL, Lai JF, Lee YK, Maynard CL, Harbour SN, Ouyang W, et al. IL-22-producing neutrophils contribute to antimicrobial defense and restitution of colonic epithelial integrity during colitis. *Proc Natl Acad Sci USA* 2013;110:12768–73.
55. Vivier E, Artis D, Colonna M, Diefenbach A, Di Santo JP, Eberl G, et al. Innate lymphoid cells: 10 years on. *Cell* 2018;174:1054–66.
56. Cibrian D, Saiz ML, de la Fuente H, Sanchez-Diaz R, Moreno-Gonzalo O, Jorge I, et al. CD69 controls the uptake of L-tryptophan through LAT1-CD98 and AhR-dependent secretion of IL-22 in psoriasis. *Nat Immunol* 2016;17:985–96.
57. Zhou L. AHR function in lymphocytes: emerging concepts. *Trends Immunol* 2016;37:17–31.
58. Benakis C, Brea D, Caballero S, Faraco G, Moore J, Murphy M, et al. Commensal microbiota affects ischemic stroke outcome by regulating intestinal gammadelta T cells. *Nat Med* 2016;22:516–23.
59. Ridaura VK, Bouladoux N, Claesen J, Chen YE, Byrd AL, Constantinides MG, et al. Contextual control of skin immunity and inflammation by corynebacterium. *J Exp Med* 2018;215:785–99.